1 For reviewer 1

Thank you for taking the time to read our paper. Your comments are appreciated and we believe that they have made the manuscript better.

The following is the author's answer to the minor comments. The *italic* text is the referee question/comment the following text is the author's answer/comment. The **(bold)** is the page - (p. #) and line number (l. #) in the document:
DIFF_Optimal_power_capture_for_wind_turbines_with_design_driving_loads.pdf
attached to this comment where the change has been highlighted.

1.) There are several grammar errors here and there. I suggest a second reading using good grammar corrector.
We have been though the paper a couple of times and the grammar should be better now.

2.) The introduction needs some revision to include more related works.
It is not clear to the authors if the referee has a specific part of the literature that he/she thought was missing?! As pointed out by another referee the work by Bottasso et al., 2010 (Multi-disciplinary constrained optimization of wind turbines) is a seminal work when talking about MDAO for wind turbine design. It is therefore added to the list of MDAO references. (**p. 2, l. 30**)
We also added the work by Buck and Garvey (2015a) discussing "thrust clipping" to the introduction. Their work was mentioned later in the paper, but it was thought that an earlier introduction would be better. (**p. 2, l. 50**)

3.) The authors assumed that the change in CT does not lead to a proportional change in CP. Can the authors elaborate more on this assumption.
It is an assumption that is a direct consequence of using 1D-momentum theory. It is best seen in equation (3) **(p. 4, l. 106)** where the classical equations for $C_T = 4a(1-a)$ and $C_P = 4a(1-a)^2$ is combined to an expression for the relationship between C_P as a function of C_T.

4.) The self-weight of the turbine is not taken into account in this study, the authors need to make this point clear in the manuscript including its impact on the general assumption used in the theory sections.
Indeed, the self-weight is not part of the optimization presented in this paper. This was mentioned in section 4.5 (Limitation of the study and possible improvements) **(p. 28, l. 415-419)**. But this is at the end of the article and as also pointed out by others the limitations of the study should have been mentioned in the introduction to make it clear for the reader which level of detail the study deals with. To accommodate this we have added a further discussion about the limitation of the study to the introduction, where the self-weight is also mentioned. **(p. 3, l. 82-87)**

5.) The 1D-aerodynamic-momentum theory is considered as a first-order theory, the authors need to discuss broadly the benefit/shortcoming of using this theory instead for example using the Blade Element Momentum theory in the rotor design.
Related to the previous comment, we have now added a further discussion about the limitations of the study to the introduction. **(p. 3, l. 66-87)** This should clarify the intent of the paper as a tool for rotor analysis in the initial stage.
Furthermore, Blade Element Momentum theory is thought to be an extension of the 1D-aerodynamic-momentum theory where losses are taken into account and the load can be varied radially as discussed in section 4.5 **(p. 28, l. 420-426)**. The authors are currently working on generalizing the method for radial load variations.

2 For reviewer 2

Thank you for taking the time to read our paper. Your comments are appreciated and we believe that they have made the manuscript better.

The following is the author's answer to the referee's questions/comments. The *italic* text is the referee question/comment the following text is the author's answer/comment. The **(bold)** is the page - (p. #) and line number (l. #) in the document :
DIFF_Optimal_power_capture_for_wind_turbines_with_design_driving_loads.pdf
attached to this comment where the change has been highlighted.

General Comment
The innovative content of the paper was not clearly stated
After rereading the introduction with this in mind the authors agree with the referee - the innovative content is not clearly stated. To make this clear we added a paragraph about where these results can be applied **(p. 2-3, l. 54-65)**. The sentence which the referee mention ("... it should be understood that the result presented here is not intended to be used directly for rotor design ..") is also taken out, as the authors meant detailed design like blade plan-form but this was not clear from the text.

Limitations in introduction
From the comment: ... *section 4.5 ... which in my opinion should be previously introduced in the introduction. This could help readers understand the real innovative content of this paper.*
The authors agree with this point and it has been accommodated by the added discussion in the introduction **(p. 3, l. 66-87)**

Additional MDAO reference
As mentioned by the referee the work by "Bottasso, Campagnolo, Croce, Multi-disciplinary constrained optimization of wind turbines, Multibody System Dynamics" is a seminal work for the use of MDAO to wind turbines and it should be part of the list of references and it is therefore added to the list of references. **(p. 2, l. 30)**

Aero-elastic extreme loads
As mentioned earlier, we have added further discussion of the limitation of the study. Here we also discuss the limitation of aero-elastic extreme loads. **(p. 3, l. 66-73)**

Minor comments
Calling C_P as "efficiency" is not correct from a theoretical stand point
The authors did not consider this fact before it was pointed out by the referee. The suggested change has been adapted **(p. 4, l. 117)**.

Equation 11: Lexp appears here for the first time but lacks of definition.
Indeed, both L_{exp} as well as $\tilde{L}$ has not been defined at this point. It is written here for later reference, which has been written in the subsequent text **(p. 7, l. 155)**.

Line 150: It should be appropriate to notices that a blade stiffness linearly proportional to the chord could be a strong approximation as the internal structure of a modern blade can be complex and could be even characterized by discontinuities.
The assumption of $EI \propto c$ is a crude approximation considering the complex structure that is a wind turbine blade. With that said, the model with $EI \propto 1/r$ is found to match fairly well with modern wind turbine blades capturing the behavior that EI becomes smaller for larger r. It is thought that the fidelity of this approximation is at least on the same order as the other models used in this study.

Line 167: I was wondering whether this assumption be really necessary. In fact, one should be interesting only in having the same (or similar) tip displacement rather than the same deformation shape of the entire blade.
It is an interesting point, and the authors did not think of this case. As the referee points out, assuming that δ_{shape} is the same when increasing R is a sufficient assumption - but it is not necessary. The more general assumption is now added to the paper **(p. 9, l. 202)**.

Figure 7 and 8: It should be mentioned that the dashed lines refers to the baseline rotor and the solid ones to the LIR rotor.
A comment about the dashed lines is now added to all the power-curves containing a baseline curve. (figure 7, 8, 10 and 11)

Figure 9: The symbol appearing in cells associated to $R_{exp} = 2$ and ΔR, ΔM_{flap} and $\Delta\delta_{tip}$ is not clear.
The authors agree that the ∞ symbol in figure 6,9 and 14 were not clear with a smaller font than the numbers. The figures have been updated together with tables in table 1, to make the content of the tables clearer.

Figure 9: In the caption: Please, consider to add also the constraint of the design for R_{exp} equal to 3 and 6, so as to provide a self-explaining figure.
We agree with the referee that this would make the figure easier to understand, and it was added to the caption.

Line 323: "But for ΔAEP it will go towards a finite value", this is not clear looking at the plot. Please, explain.
&
It is not straightforward to understand why for many conditions the "Δ"-quantities go to infinity. I may suggest to add an explanation.
There is indeed no explanation for the limiting cases when $R_{exp} \to 2$. The authors agree that it was confusing not to mention why this is the case. We have added a comment that the result is found by investigating the limit $R_{exp} \to 2$. **(p. 14, l. 281)(p. 17, l. 346)(p. 22, l. 387)(p. 27, l. 405)**. The explanation for this case was thought to be "complicated" and that it would overshadow the results. Especially considering that this limit is not of much practical value. We have attached a separate pdf appendix to this comment ("Limit_Rexp->2.pdf") where the limit values are found for all the three optimization case. We do not plan to add this appendix to the article since it is thought to complicate the understanding of the paper.

Caption of Fig. 13: "It is a similar plot to figure 5 but here it is for the AEP-optimized rotor and it is the change in the max load.". The sentence is not clear.Please, rephrase.
After rereading the caption the authors agree and the sentence is hard to interpret. It was rephrased. **(p. 25, fig. 13)**

Section 4.4 contains only the table and just a sentence. Consider the possibility to insert that content in a previous or subsequent section, or to extend the text with some comments.
The authors added some comments to the section comparing the three optimization methods. **(p. 27, l. 401-407)**

Line 388: "In spite of relatively ... thrust clipping": the concept express in this sentence may be anticipated in the introduction within the context of the innovative content of work.
A paragraph mentioning the concept of thrust-clipping and the study by Buck and Garvey (2015a) was added to the introduction. **(p. 2, l. 47-53)**

Line 394: I agree with the possible inclusion of the radial variation of rotor loading, but what

about the use of a more realistic relationship between C_P and C_T? In fact a wind turbine may operate close to $CT = 8/9$ but far from the Betz optimal C_P
It is true that in practice a wind turbine will not reach close to Betz-limit. This is often a consequence of a non-constantly loaded rotor - which is an assumption in this study. For a non-constantly loaded rotor, the loads are not directly related thought C_T and R and the method in this study can not directly be applied. The authors are currently working on generalizing the framework for the radially varying case.

Optimal relationship between power and design driving loads for wind turbine rotors using 1D models

Kenneth Loenbaek[1,2], Christian Bak[2], Jens I. Madsen[1], and Bjarke Dam[1]

[1]Suzlon Blade Science Center, Havneparken 1, 7100 Vejle, Denmark
[2]Technical University of Denmark, Frederiksborgvej 399, 4000 Roskilde, Denmark

Correspondence: Kenneth Loenbaek (kenneth.loenbaek@suzlon.com)

Abstract. We investigate the optimal relationship between the aerodynamic power, thrust loading, and size of a wind turbine rotor when its design is constrained by a static aerodynamic load. Based on 1D-axial momentum theory, the captured power $\tilde{P}$ for a uniformly loaded rotor can be expressed in terms of the rotor radius R and the rotor thrust coefficient C_T. Common types of static Design Driving Load Constraints (DDLC), e.g. limits on the permissible root-bending moment or tip deflection, may be generalized into a form that also depends on C_T and R. The developed model is based on simple relations and make explorations of overall parameters possible in the early stage of the rotor design process. Using these relationships to maximize $\tilde{P}$ subject to a DDLC, shows that operating the rotor at the Betz limit (maximum C_P) does not lead to the highest power capturepower-capture. Rather, it is possible to improve performance with a larger rotor radius and lower C_T without violating the DDLC. As an example, a rotor design driven by a tip-deflection constraints, constraint may achieve 1.9% extra power capture power-capture $\tilde{P}$ compared to the baseline (Betz limit) rotor.

The method is extended for optimization of rotors with respect to Annual Energy Production (AEP), where the thrust characteristics $C_T(V)$ needs to be determined together with R. This results in a much higher relative potential for improvements , since the constraint limit can be met over a larger range of wind speeds. For example, a relative gain in AEP of +5.7% is possible for a rotor design constrained by tip deflections compared with a rotor designed for optimal C_P. The optimal solution for AEP leads to a thrust curve with three distinct operational regimes and so called so-called thrust-clipping.

Keyword: Wind Energy, Wind Turbine, Initial rotor design, Low Induction Rotor, Thrust-clipping, Peak-shaving

1 Introduction

Since the start From the inception of the wind energy industry, it has been a clear trend that the rotor size is increasing. But as it has been rotor sizes are increasing. However, as discussed in Sieros et al. (2012)the increasing , increasing the rotor size is not a clear way to decrease the Cost of Energy (CoE), since the weight (which is rotor weight (closely related to cost) of the rotor always will rotor cost) will always scale with a higher exponent than the increase in power does. It is therefore argued that the lower CoE, that has taken place, is mostly due to technology improvements. The structural design of the turbine is built to carry the loads coming from the aerodynamics (steady or extreme) and the self weightself-weight. Therefore lowering the loads should lead to a lighter blade. The steady aerodynamic load is applied in order to extract power and increasing the load leads to a higher power until ~~maximum power efficiency~~ the maximum power coefficient (max C_P) is reached. Increasing the load should lead to a heavier blade but it also leads to ~~a~~ higher power production. It goes to show that understanding the relationship between loading, power production and structural response is very important to get the most ~~cost effective~~ cost-effective turbine. It follows a trend that has been in the recent ~~year~~ years that wind turbine optimization should include a more holistic approach with concepts like Multidisciplinary Design Analysis and Optimization (MDAO) and System Engineering ~~(Fleming et al., 2016; Perez-Moreno et al., 2016; Zahle et al., 2015)~~ (Bottasso et al., 2010; Zahle et al., 2015; Fleming et al., 2016; Perez-

here all the parts of the turbine design that affect the cost should be taken into account with the overall objective of minimizing CoE. Some of these related works focus more on how the rotor loading affects the power and the ~~relationship between rotor loading effect on power and~~ structural response. One of the concepts that ~~comes~~ come out of it is the ~~so called~~ so-called ~~*Low Induction Rotor*~~*Low-Induction-Rotor* (LIR) where the velocity induction at the rotor plane is lower than the value that maximizes the power ~~efficiency~~coefficient. The concept was introduced by Chaviaropoulos and Sieros (2014) where it comes out of optimizing Annual Energy Production (AEP) by allowing the rotor to grow while constraining the flap root bending moment to be the same as a baseline. They state that the method can increase the AEP with 3.5% with a 10% increase in the rotor radius hereby showing that LIR can increase AEP while keeping the same flap root bending moment. It agrees with Kelley (2017) who allowed for a change in the radial loading resulting in an AEP increase of 5% with a radius increase of 11%. It was also investigated by Bottasso et al. (2015) where they both tested the potential of using LIR for AEP improvements with load constraint as well as a ~~cost optimized~~ cost-optimized rotor. They find the same as the previous two investigations that LIR can improve AEP, but when they consider the CoE they find the LIR is not ~~cost effective~~cost-effective, meaning that the additional cost of extending the blade is not compensated by the increase in power. This conclusion is opposed to the conclusion made by Buck and Garvey (2015b) where they target to minimize the ratio between Capital Expenditures (CapEx) and AEP. They arrive at LIR as the optimal solution for CapEx/AEP which is taken as a measure for CoE. Overall it seems that LIR can increase AEP while keeping the same load as a non-LIR baseline, but it is not clear if LIR is a ~~cost effective~~ cost-effective solution.

Another concept that is relevant in the context of this paper is Thrust-Clipping (also known as peak-shaving or force-capping). For turbines, it is often the case that the maximum thrust is reached just before rated power resulting in a so-called thrust peak. When using thrust-clipping this peak is lowered at the cost of power. It is used for many contemporary turbines for load alleviation, but is often added as a feature after the design process. Buck and Garvey (2015a) made a design study where they found that lowering the maximum thrust by 11% leads to 9% reduction in material content, at the cost of 0.1% lifetime energy, resulting in an overall reduction of 0.2% in cost of energy. Which shows that including thrust-clipping in the design process can lead to a lower CoE.

In this paper, we investigate the relationship between load, power and structural response ~~. We will use simple analytical model like~~ of wind turbine rotors. Simple analytical models, based on 1D-aerodynamic-momentum theory and Euler-Bernoulli-Beam theory~~which is rather crude approximations to use for wind turbine~~ , are introduced to establish the first order relationship between these responses. This provides a useful framework for initial rotor design, ~~but it should be understood that the result presented here is not intended to be used directly for rotor design but to show a possible way to include structural/loadconstraints into the design process. Instead of using a cost model we make constraints on the load~~e.g. when high level design parameters such as the rotor radius need to be fixed or to understand how load/~~structural response relative to a baseline design and require that the~~ structural responses will change with rotor size. The effect on the power curve and the related load/structural response ~~is not larger than the baseline. As it was argued above, keeping the same load does not necessary mean that the cost of the blade is the same and it is a limitation of the work. A better measure for the blade cost is to keep the mass constant, and a constraint was setup where the mass of~~ with the variation in wind speeds is also investigated, which is useful for initial design of the highly coupled Aero-Servo-Elastic rotor design problem.

The relatively simple models used in this paper do not capture the full complexity needed for detailed wind turbine rotor design and should be considered a tool for early stage rotor design and overall exploration only. For example, the ~~load carrying part of blade was kept to get a likely better constraint for an equal cost . The constraints will not include the effect from aero-elastic extreme loads as it~~ underlying theories (of 1D-aerodynamic-momentum and Euler-Bernoulli beams) assume steady-state conditions, while designs are often constrained by load cases that are linked with extreme, unsteady, or non-normal operational events, e.g. extreme turbulence, gusts, emergency shutdowns, subsystem faults, or parked conditions. This is a limitation of the developed model, but if there is a relation between the steady-state loads and the extreme loads, which is very likely, then the results are still valid.

As mentioned before, the overall target for current turbine design is to lower the CoE, but a cost model is not used, which is also a limitation of this study. However, cost models relate to several assumptions made in the design process such as the price of components in the design or composite lay-up of the blades, so a predicted cost will always be made with some uncertainty. Instead, load constraints are considered, much like for the above-mentioned Low-Induction-Rotor (LIR) example. As it was found by Bottasso et al. (2015), a constrained load might not lead to a lower CoE. So to accommodate for this, a constraint with fixed mass is made, which is thought to be ~~out of scope for an analysis at this level. But it is expected that if the extreme loads happens in normal operation there should be a relationship between the steady and extreme loads.~~ a better approximation for a fixed cost.

~~The paper starts by presenting the background , then continues to present the which leads into~~ This study is carried out to obtain an overview of how the rotor design more fundamentally is influenced by different types of aerodynamic loading. Thus, an issue like the "self-weight" is important for modern turbines, but is not directly included in this study; especially the static-mass-moment has an impact on contemporary turbines. It could be included, but it was excluded to keep the study as simple as possible. Further discussion about the limitations and possible improvements of the study is given later in section 4.5.

2 Theory

This section will introduce the variables and the basic relationships used in this paper. It is split into two subsections: where subsection 2.1 introduces aerodynamic variables, equations, as well as the baseline rotor, while the second subsection 2.2 present scaling laws used to formulate design driving load constraints relative to the baseline rotor.

2.1 Aerodynamics

The theory for this Aerodynamics section is found in Sørensen (2016).

For wind turbine aerodynamics non-dimensional coefficients are often introduced and some of the common ones are for the rotor thrust (C_T) and power (C_P).

$$C_T = \frac{T}{\frac{1}{2}\rho V^2 \pi R^2} \tag{1}$$

$$C_P = \frac{P}{\frac{1}{2}\rho V^3 \pi R^2} \tag{2}$$

Where T and P are the rotor thrust and power respectively, ρ is the air density, V is the undisturbed flow speed and R is the rotor radius.

These definitions can be applied for any wind turbine rotor, but in this paper, we will use a simplified relationship between C_T and C_P, which is derived from classical 1D-momentum theory. This implies an assumption of uniform aerodynamic loading across the rotor plane. The classical equations are often given in terms of the axial induction (a), which is defined as $a = 1 - \frac{V_{rotor}}{V}$ where V_{rotor} is the axial flow speed in the rotor plane. By combining the two classical momentum theory expressions for $C_P(a)$ and $C_T(a)$ (Sørensen, 2016, p. 11 eq. 3.8), the following relationship between these coefficients is arrived at:

$$\left.\begin{aligned} C_T(a) &= 4a(1-a) \\ C_P(a) &= 4a(1-a)^2 \end{aligned}\right\} \implies C_P(C_T) = (1-a)C_T = \frac{1}{2}\left(1+\sqrt{1-C_T}\right)C_T, \quad C_T \in [0,1[\tag{3}$$

Where $a(C_T)$ is found by inverting $C_T(a)$ and using the negative solution. A plot of C_T vs. C_P can be seen in figure 1. This $C_P(C_T)$ curve is monotonically decreasing in slope and reaches a maximum $C_P = 16/27$ corresponding to the well-known Betz-limit at $C_T = 8/9$. These ~~monotoncity properties leads~~ monotonicity properties lead to the key observation that a reduction in thrust ($C_T = 8/9 - \Delta C_T$) will not lead to a proportional change in power (ΔC_P). This motivates this paper's investigation of the trade-off between power and ~~load~~loads.

~~Power capture~~ Power-capture and Annual Energy Production (AEP)

One way to understand the power yield of a rotor is to consider equation 2 as consisting of three separate terms:

$$P = \underbrace{\frac{1}{2}\rho V^3}_{\text{Wind}} \cdot \underbrace{\pi R^2}_{\text{Size}} \cdot \underbrace{C_P}_{\text{~~Efficiency~~Coefficient}} \tag{4}$$

Wind is the part of the equation that depends on the wind conditions, *Size* is the part of the equation that depends on the rotor swept area, and ~~*Efficiency*~~*Coefficient* is ~~how much of the potential power the rotor can extract from the kinetic power of~~ the part of the equation related to the power coefficient, representing the capability of the rotor to extract power from the wind. The combination of equations 2 and 3 provides an expression that captures the latter two terms, which are the only ones affected

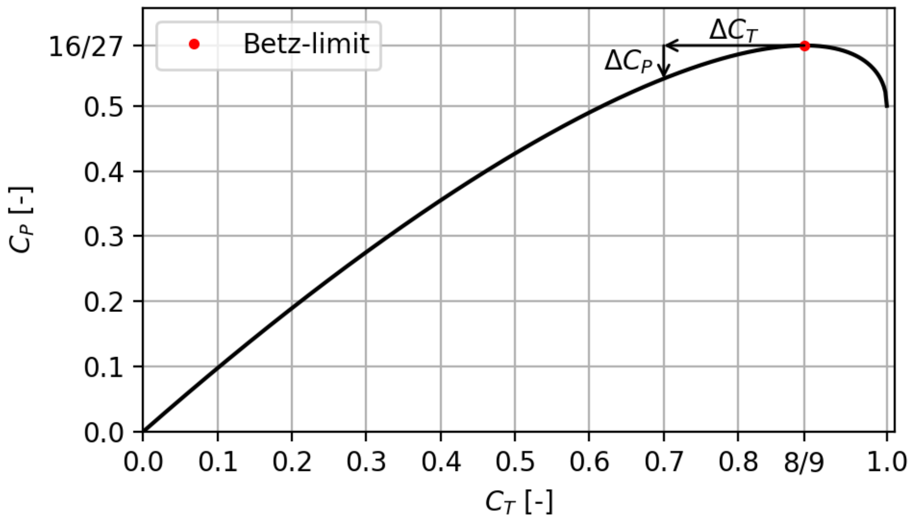

Figure 1. Relationship between normalized rotor load C_T and power ~~efficiency~~ coefficient C_P from one-dimensional momentum theory. Notes that around Betz-limit a small change in C_T does not lead to a proportional change in C_P, this is illustrated by ΔC_T and ΔC_P.

by the design of the turbine:

$$\tilde{P}(C_T,\tilde{R}) = \frac{P}{\frac{1}{2}\rho V^3 \pi R_0^2} = C_P \tilde{R}^2 = \frac{1}{2}\left(1+\sqrt{1-C_T}\right) C_T \tilde{R}^2 \quad (5)$$

Where $\tilde{R}$ equals R/R_0, with R_0 being the radius of the baseline rotor. This equation will be referred to as the ~~*Power Capture*~~*Power-Capture* equation. It shows that power can be changed by changing either the loading (C_T) or the rotor radius (R). This will serve as the basic equation when the ~~power capture~~ power-capture is optimized for a single design point.

When considering turbine design over the range of operational conditions, the *Annual Energy Production* (AEP) is introduced as an integral metric stating the energy produced per year given some wind speed frequency distribution. It can be computed as the power production (P) weighted by the probability density of wind speeds (PDF_{wind}) multiplied by the period of one year (T_{year}):

$$AEP = T_{year}\frac{1}{2}\rho\pi R_0^2 \int_{V_{CI}}^{V_{CO}} \tilde{P}(C_T(V),\tilde{R}) \cdot V^3 \cdot PDF_{wind}(V) dV \quad (6)$$

The wind speed probability distribution PDF_{wind} will be described with a Weibull distribution. V_{CI} and V_{CO} is the wind speed for *Cut In* and *Cut Out* for wind turbine operation. Here they are taken to be $V_{CI} = 3\text{ms}^{-1}$ and $V_{CO} = 25\text{ms}^{-1}$, which is common numbers for modern wind turbines.

In this paper, we will use a dimensionless measure for AEP which is equivalent to the ~~so called~~ so-called capacity factor, defined as follows:

$$A\tilde{E}P(C_T,\tilde{R}) = \frac{AEP}{T_{year}P_{rated}} = \frac{AEP}{T_{year}\frac{1}{2}\rho\pi R_0^2\frac{16}{27}V_0^3} = \frac{27}{16}\int\limits_{\tilde{V}_{CI}}^{\tilde{V}_{CO}} \tilde{P}(C_T(\tilde{V}),\tilde{R})\cdot\tilde{V}^3\cdot PDF_{wind}(\tilde{V})d\tilde{V} \tag{7}$$

$\tilde{V}$ is a normalized wind speed given as $V=\tilde{V}V_0$ where V_0 is the wind speed at which the turbine reach rated power. In all of this paper it is taken to be $V_0 = 10\mathrm{ms}^{-1}$. It should further be noted that $PDF_{wind}dV$ is dimensionless and non-dimensionalizing the AEP it also follows that $PDF_{wind}d\tilde{V}$ is dimensionless. In all of this paper $A\tilde{E}P$ is computed by discretization of the integral and computing the integral with the trapezoidal rule given as $\int_{\tilde{V}_{CI}}^{\tilde{V}_{CO}} f(\tilde{V};C_T,\tilde{R})d\tilde{V} \approx \sum_{i=1}^{N}\frac{f(\tilde{V}_{i+1};C_T,\tilde{R})+f(\tilde{V}_i;C_T,\tilde{R}))}{2}\Delta\tilde{V}_i$ where the discretization (N) was found to become insignificant with $N=200$.

Baseline rotor

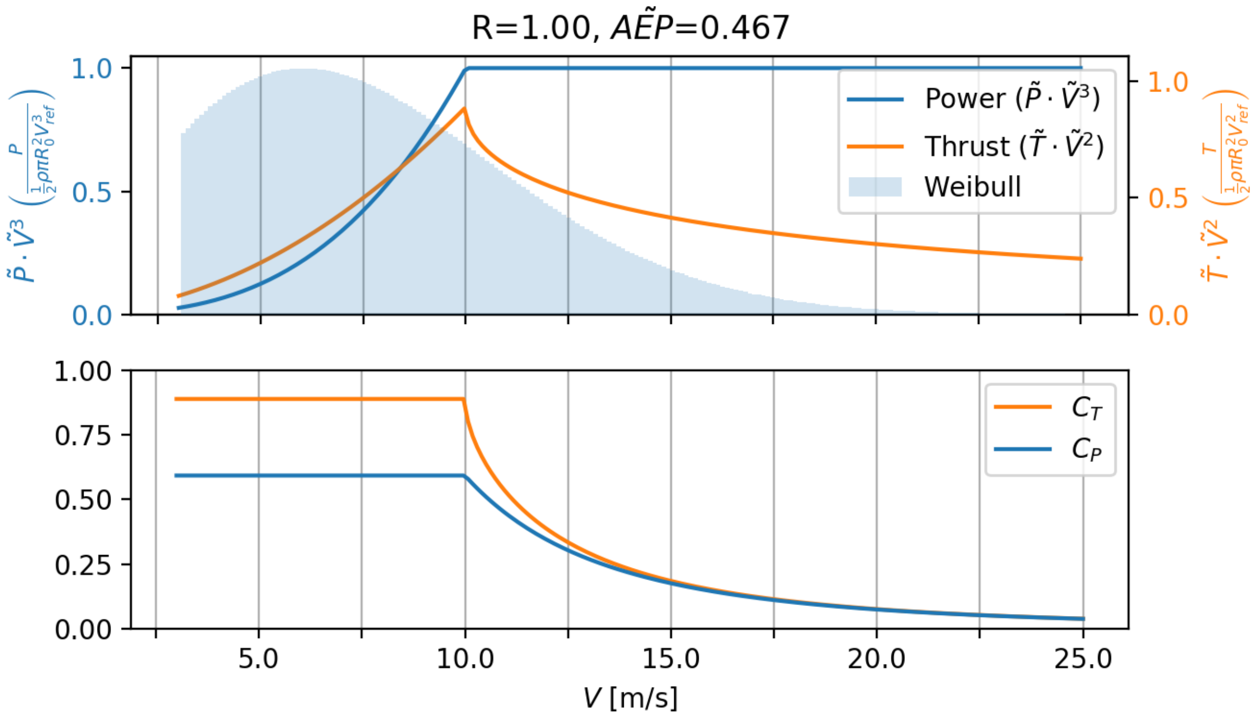

Figure 2. Top: The dimensionless power and thrust for the baseline rotor as a function of wind speed. Overlaid (in blue) the Weibull wind speed frequency distribution used throughout (IEC-class III: $V_{avg}=7.5$, $k=2$). Bottom: C_T and C_P as a function of wind speed. These curves reflect how most turbines are operated today, targeting maximum power ~~efficiency~~ coefficient below rated power, which leads to a thrust peak just before rated power.

The work here aims at demonstrating improved rotor performance compared to a baseline design. This baseline design is chosen to be a turbine operating at the Betz-limit below rated wind speed and keeping a constant power above rated.

$$C_{T,0} = \frac{8}{9} \approx 0.889, \qquad C_{P,0} = \frac{16}{27} \approx 0.593 \tag{8}$$

This choice of baseline mimics the typical practice of designing wind turbines to target operation with maximum C_P below rated power. In reality, turbines will not achieve maximum C_P at $C_T = 8/9$ since losses alter the relationship between C_T and C_P, but this does not change the fact that turbines are operated at the point of maximum C_P. Figure 2 shows the power and thrust curves for the baseline rotor.

In this paper, all results presented as the change in performance relative to that of the baseline rotor. For this reason, all the relevant variables will be normalized by the corresponding baseline rotor values.

$$\Delta R = \frac{R}{R_0} - 1 \tag{9}$$

$$\Delta \tilde{P} = \frac{C_P R^2}{C_{P,0} R_0^2} - 1 \tag{10}$$

$$\Delta \tilde{L} = \frac{C_T R^{L_{exp}}}{C_{T,0} R_0^{L_{exp}}} - 1 \tag{11}$$

$$\Delta A\tilde{E}P = \frac{A\tilde{E}P}{A\tilde{E}P_0} - 1 \tag{12}$$

where $\tilde{L}$ as well as L_{exp} is a generalized load that ~~will be introduced in the next subsection~~is introduced in section 4.1 *(Effects on loads)* and it is written here for later reference.

2.2 Scale laws and constraints for Design Driving Loads

In this section, examples of static aerodynamic *Design Driving Loads* (DDL) will be presented. These examples are not meant to be exhaustive ~~,~~ but include several of the key considerations that constrain the practical design of wind turbine rotors. From the scaled loads, *Design Driving Load Constraints* (DDLC) are introduced, which limit loads so that these do not exceed the levels of the baseline rotor. Based on the DDL examples, it is shown that DDLCs can be elegantly put in a generalized form.

Thrust (T)

Thrust typically does not limit the design of the rotor itself, but more likely is a constraint imposed from the design of the tower and/or foundation. The thrust scaling and the associated DDLC is given by:

Scaling $\qquad\qquad$ DDLC

$$T = \frac{1}{2}\rho V_0^2 \pi R^2 C_T \quad \Longrightarrow \quad \mathrm{DDLC}(T) = \frac{T}{T_0} = \frac{C_T}{C_{T,0}}\left(\frac{R}{R_0}\right)^2 \leq 1 \tag{13}$$

Root flap bending moment (M_{flap})

The root flap moment is the bending moment at the rotational center in the axial flow direction. To compute M_{flap}, the 1D-momentum-theory relations for infinitesimal thrust (dT) and moment (dM) are integrated:

$$\mathrm{d}T = \frac{1}{2}\rho V^2 C_T 2\pi r \mathrm{d}r \tag{14}$$

$$\mathrm{d}M_{flap} = r\mathrm{d}T \tag{15}$$

Where r is the radius location of the infinitesimal load ($r \in [0, R]$). The moment scaling and DDLC can ~~therefore~~ be found as:

Scaling / DDLC

$$M_{flap} = \int_0^R \mathrm{d}M_{flap} = \frac{1}{3}\rho V_0^2 C_T \pi R^3 \quad \Longrightarrow \quad \mathrm{DDLC}(M_{flap}) = \frac{M_{flap}}{M_{flap,0}} = \frac{C_T}{C_{T,0}}\left(\frac{R}{R_0}\right)^3 \leq 1 \tag{16}$$

As it is seen M_{flap} scales with R^3 so it ~~grow~~ grows faster than the power, which grows as R^2. M_{flap} is important for the blade design since the flap-wise aerodynamic loads need to be transferred via the blade structure to the root of the blade.

Tip deflection (δ_{tip})

Tip deflection is a common DDLC for contemporary utility-scale turbines, where tip clearance between tower and blade may become critical because of relatively long and slender blades. To get an idea for how tip-deflection scales with changes in loading and rotor radius, Euler-Bernoulli Beam Theory (Bauchau and Craig, 2009, p. 189 eq. 5.40) is used. For the problem here it takes the form:

$$\frac{\mathrm{d}^2}{\mathrm{d}r^2} EI \frac{\mathrm{d}^2\delta}{\mathrm{d}r^2} = \frac{\mathrm{d}T}{\mathrm{d}r} = \frac{1}{2}\rho V^2 C_T 2\pi r \tag{17}$$

Where δ is the deflection in the flap-wise direction of the blade at location r. EI is the stiffness of the blade ~~a~~ at location r. For modern turbines the stiffness decrease towards the tip of the blade. To get an estimate for the stiffness it is assumed that stiffness follows the size of the chord ($EI \propto c$). The chord is given by the equation in (Sørensen, 2016, p. 68 eq. 5.26) with an approximation for the outer ~~most~~ part of the blade it can be found that $c \propto R/r$ which means that $EI \propto R/r$. An approximate model for EI can be made that have $EI \propto R/r$:

$$EI(r) = \frac{EI_r}{1 + \left(\frac{EI_r}{EI_t} - 1\right)\frac{r}{R}} \tag{18}$$

Where EI_r is the stiffness at the root and EI_t is the stiffness at the tip of the blade. As mentioned above for wind turbines $EI_r > EI_t$.

With the equation for EI equation 17 can be solved by indefinite integration where the integration constants are determined from the following boundary conditions:

$$\underbrace{\delta(r=0) = 0, \quad \frac{\mathrm{d}\delta}{\mathrm{d}r}(r=0) = 0}_{\text{Clamped root}} \qquad \underbrace{\frac{\mathrm{d}^2\delta}{\mathrm{d}r^2}(r=R) = 0, \quad \frac{\mathrm{d}^3\delta}{\mathrm{d}r^3}(r=R) = 0}_{\text{Free tip}} \tag{19}$$

The resulting displacement solution looks the followingbecomes:

$$\delta = \frac{11\pi}{120}\frac{V^2\rho}{EI_r}C_T R^5\left(\frac{2}{33}\left(\frac{EI_r}{EI_t}-1\right)\tilde{r}^6+\frac{1}{11}\tilde{r}^5-\frac{5}{11}\left(\frac{EI_r}{EI_t}-1\right)\tilde{r}^4+\frac{10}{11}\left(\frac{2}{3}\frac{EI_r}{EI_t}-\frac{5}{3}\right)\tilde{r}^3+\frac{20}{11}\tilde{r}^2\right) \tag{20}$$

$$= \frac{11\pi}{120}\frac{V^2\rho}{EI_r}C_T R^5\delta_{shape}\left(\tilde{r},\frac{EI_r}{EI_t}\right) \tag{21}$$

Where the normalized radius ($\tilde{r}\in[0,1]$) has been introduced so that $r = R\cdot\tilde{r}$. The maximum deflection occurs at the blade tip ($\tilde{r}=1$), which leads to the following scaling relation and DDLC for tip deflection:

Scaling | DDLC

$$\delta_{tip} = \frac{11\pi}{120}\frac{V^2\rho}{EI_r}C_T R^5\delta_{shape}\left(\tilde{r}=1,\frac{EI_r}{EI_t}\right) \quad\Longrightarrow\quad \mathrm{DDLC}(\delta_{tip}) = \frac{\delta_{tip}}{\delta_{tip,0}} = \frac{C_T}{C_{T,0}}\left(\frac{R}{R_0}\right)^5 \le 1 \tag{22}$$

Where it implicitly has has implicitly been assumed that any change in stiffness needs to follow:

$$\frac{EI_r}{EI_t} = \frac{EI_r}{EI_{r,0}}\left(\frac{EI_{r,0}}{EI_{t,0}}+\frac{26}{7}\right)-\frac{26}{7} \tag{23}$$

With the simplest way to satisfy this relation being that $EI_r = EI_{r,0}$ which gives $\frac{EI_r}{EI_t} = \frac{EI_{r,0}}{EI_{t,0}}$ so that δ_{shape} is not changed when R is increased.

Tip deflection with constant mass

The final example of a DDL is also based on tip deflection , but includes a condition to maintain a constant mass of the load carrying load-carrying structure of the blade. To this end the stylized spar-cap layout depicted in figure 3 is assumed. This layout consists of two planks. The stiffness of a spar-cap structure with homogeneous Young's-modulus (E) can be found from the stiffness of a rectangle and the parallel axis theorem (see figure 3 for variable definition):

$$\left.\begin{aligned} I_{rect} &= \frac{Bh^3}{12} \\ EI &= 2E\left(I_{rect}+A\left(\frac{H-h}{2}\right)^2\right) \\ A &= Bh \end{aligned}\right\} EI = 2E\left(\frac{Bh^3}{12}+Bh\left(\frac{H-h}{2}\right)^2\right) = \frac{H^2Bh}{2}\left(\frac{h^2}{3H^2}+\left(1-\frac{h}{H}\right)^2\right) \tag{24}$$

For modern wind turbines $h/H << 1$ meaning that a common approximation is:

$$EI \approx E\frac{H^2Bh}{2} \tag{25}$$

To compute the mass for such a structure it will be assumed that plank height h and the plank width B is constant and that the change in EI comes from a decrease in building height H. If then h is decreased when R is increased the following relationship need needs to be satisfied in order for the mass of the planks to have constant mass (assuming constant mass density):

$$Rh = R_0h_0 \tag{26}$$

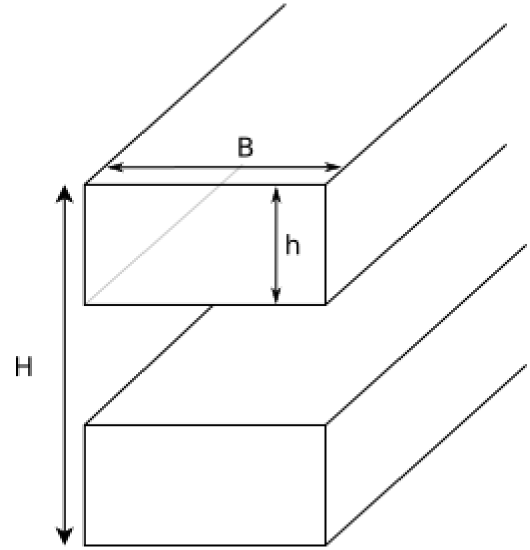

Figure 3. Assumed spar-cap structure with dimensions: H is the total build height, h is the space between planks, and B is the plank width.

From there it follows that changes in the radius of the rotor will ~~changes~~ change the stiffness as:

$$\left.\begin{aligned} EI &\approx E\frac{H^2Bh}{2} \quad (25)\\ h &= \frac{R_0h_0}{R} \quad (26)\end{aligned}\right\} EI \approx E\frac{H^2BR_0h_0}{2R} \tag{27}$$

Combining the equation with the tip deflection equation (21) the following scaling and DDLC can be found:

$$\begin{array}{ccc} \text{Scaling} & & \text{DDLC} \\ \left.\begin{aligned} \delta_{tip} &= \frac{11\pi}{120}\frac{V^2\rho}{EI_r}C_TR^5\delta_{shape}\left(\tilde{r}=1,\frac{EI_r}{EI_t}\right) \\ EI &\approx E\frac{H^2BR_0h_0}{2R}\end{aligned}\right\} & \Longrightarrow & \text{DDLC}(\delta_{tip+mass}) = \frac{C_T}{C_{T,0}}\frac{EI_{r,0}}{EI_r}\left(\frac{R}{R_0}\right)^5 = \frac{C_T}{C_{T,0}}\left(\frac{R}{R_0}\right)^6 \leq 1 \end{array} \tag{28}$$

Where it has been used that changing h by the same magnitude for the whole blade leads to $\frac{EI_r}{EI_t} = \frac{EI_{r,0}}{EI_{t,0}}$ and hereby not affecting δ_{shape}. It should be noted that by choosing B to change instead will lead to the same scaling, but with the difference being that changing the plank thickness might lead to ~~higher order~~ higher-order effects, although they are expected to be insignificant.

Generalizing the constraint form

Considering the four DDLC examples presented above, there appears to be a pattern in the scaling relations that may be written as follows:

$$\frac{C_T}{C_{T,0}}\left(\frac{R}{R_0}\right)^{R_{exp}} \leq 1 \tag{29}$$

Where R_{exp} is the *DDLC R-Exponent*.
If the constraint limit is met the following relationship can be written as:

$$R = R_0\left(\frac{C_{T,0}}{C_T}\right)^{\frac{1}{R_{exp}}} \tag{30}$$

3 Formulation of rotor design problems

Based on the performance and constraint relationships outlined in the previous section, this section will present the formulation ~~of~~ for rotor design as optimization problems. Two different classes of problems are introduced, namely: ~~*Power Capture*~~ *Power-Capture optimization* and *AEP optimization*, where the latter is a generalization of the former with the constraint depending on wind speed.

3.1 ~~Power Capture~~ Power-Capture optimization

The optimization problem can be stated as:

$$\underset{C_T,\tilde{R}}{\text{maximize}} \quad \tilde{P} = \frac{1}{2}\left(1+\sqrt{1-C_T}\right)C_T\tilde{R}^2 \tag{31}$$

$$\text{subject to} \quad \frac{C_T}{C_{T,0}}\tilde{R}^{R_{exp}} \leq 1 \tag{32}$$

Where the definition of $\tilde{R} = R/R_0$ has been used for consistency . The solution for this optimization problem is presented in the 4.1 section.

It should be noted that this optimization problem is similar to the problem that is given by Chaviaropoulos and Sieros (2014) where they optimize while keeping M_{flap}. So the optimization problem in this paper is a generalization of their optimization problem.

3.2 AEP optimization

In contrast to the above mentioned optimization of ~~power capture~~power-capture, optimization with respect to AEP requires to determine $C_T(\tilde{V})$ so a function opposed to a scalar value. It is also necessary to fix the rated power to a constant value, while the wind speed at which rated power is reached is allowed to change. The problem can be formulated as:

$$\underset{C_T(\tilde{V}),\tilde{R}}{\text{maximize}} \quad A\tilde{E}P = \frac{27}{16}\int_{\tilde{V}_{CI}}^{\tilde{V}_{CO}} \tilde{P}(C_T(\tilde{V}),\tilde{R})\cdot\tilde{V}^3\cdot PDF_{wind}(\tilde{V})d\tilde{V} \tag{33}$$

$$\text{subject to} \quad \begin{aligned} &\tilde{V}^2\frac{C_T(\tilde{V})}{C_{T,0}}\tilde{R}^{R_{exp}} \leq 1, \quad \text{(DDLC)} \\ &\frac{27}{16}\tilde{P}(C_T(\tilde{V}),\tilde{R})\tilde{V}^3 \leq 1, \quad \text{(rated power)} \end{aligned} \tag{34}$$

Where the the wind speed scaling has been added to the DDLC.

4 Results and discussion

This section discusses the solutions ~~of~~ to the rotor design optimization problems introduced in the previous section.

4.1 Optimizing for ~~power capture~~power-capture

The constrained optimization problem to maximize ~~power capture~~power-capture, as stated in ~~the~~ section 3, may be simplified based on the observation that optimum solutions will occur at the DDL constraint limit. To understand this, consider that the ~~power capture~~ power-capture of a rotor with an inactive constraint may always be improved by growing the rotor until the constraint is met. This is true irrespective of what DDLC that determines the rotor design. Hence, an explicit relation $\tilde{R}(C_T)$ can be used to reformulate from a constrained optimization problem in two variables to an unconstrained optimization problem in one variable.

$$\left.\begin{aligned} \tilde{P}(C_T,\tilde{R}) = \frac{1}{2}\left(1+\sqrt{1-C_T}\right)C_T\tilde{R}^2 \quad (5) \\ \tilde{R} = \left(\frac{C_{T,0}}{C_T}\right)^{\frac{1}{R_{exp}}} \quad (30) \end{aligned}\right\} \implies \tilde{P}(C_T) = \frac{C_{T,0}^{2\frac{1}{R_{exp}}}}{2}\left(1+\sqrt{1-C_T}\right)C_T^{1-2\frac{1}{R_{exp}}} \tag{35}$$

With the optimization problem now being:

$$\underset{C_T}{\text{maximize}} \quad \tilde{P} = \frac{C_{T,0}^{2\frac{1}{R_{exp}}}}{2}\left(1+\sqrt{1-C_T}\right)C_T^{1-2\frac{1}{R_{exp}}} \tag{36}$$

By differentiating the objective function 35 with respect to C_T and finding its root, the optimal C_T as a function of R_{exp} is arrived at:

$$\frac{d\tilde{P}(C_T)}{dC_T} = 0 \implies \tag{37}$$

$$C_T = \frac{8\left(R_{exp}^2 - 3R_{exp} + 2\right)}{\left(3R_{exp} - 4\right)^2} \tag{38}$$

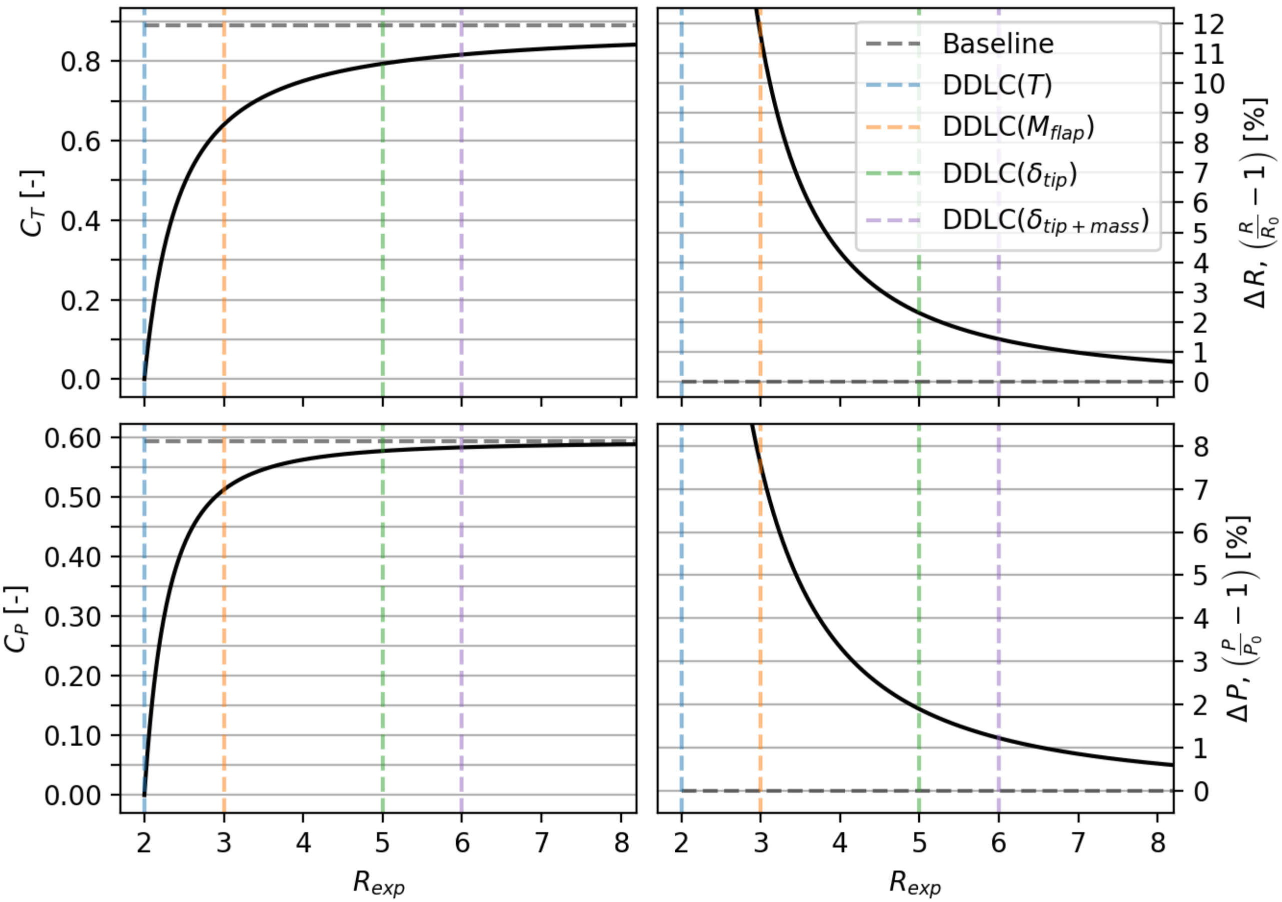

Figure 4. Top left: Optimal C_T as a function of the constraint R-exponent (R_{exp}). Low left: R_{exp} vs. C_P, notice that the optimal C_P curve has a steeper slope and hugs the baseline closer than C_T. Top right: R_{exp} vs. relative change in radius ΔR. Lower right: R_{exp} vs. relative change in ~~power capture~~ power-capture ($\Delta \tilde{P}$). Despite the similar shape of curves a difference between the two is that $\Delta P(R_{exp} \to 2) = 50\%$ where $\Delta R(R_{exp} \to 2) \to \infty$. The vertical lines represent each of the example constraints. (*DDLC=Design Driving Load Constraint*).

$$\frac{d\tilde{P}(C_T)}{dC_T} = 0 \implies$$

$$C_T = \frac{8\left(R_{exp}^2 - 3R_{exp} + 2\right)}{\left(3R_{exp} - 4\right)^2}$$

This unique solution is a maximum, which is apparent from the always positive signs of ΔP in figure 4. This figure shows the optimal solution for C_T and C_P, as well as the relative change in radius (ΔR) and power (ΔP) compared to the baseline rotor. From the two left plots, C_P is observed to approach the dashed baseline performance (Betz rotor) much faster than C_T

as R_{exp} increases. This is a consequence of the relationship between C_T and C_P (figure 1). Especially around the Betz-limit, the gradient is very small, which means that changes in C_T does do not lead to proportional changes in C_P. Turning to the two plots on the right in figure 4, it is seen that the lower C_P is more than compensated by increasing R since the relative change in power (ΔP) is always positive.

When maximizing power capture power-capture for a given thrust ($R_{exp} = 2$) $R_{exp} = 2$; blue dashed vertical line in figure 4), it is seen that the impractical solution of an infinitely large rotor with low aerodynamic loading results found that $C_T \to 0$ and $\Delta R \to \infty$ while $\Delta P \to 50\%$, which was found by investigating the limit value behavior when $R_{exp} \to 2$. Since $\Delta R \to \infty$ is not of much practical interest, further explanation is not given here. Alternatively, the maximum power for a given flap root moment ($R_{exp} = 3$; orange line) may be achieved by increasing the rotor radius by 11.6% compared to the baseline design (maximum C_P). The corresponding relative increase in power ΔP is 7.6%. Finally, designs constrained by tip-deflection ($R_{exp} = 5$; green line) allow allows the relative power ΔP to increase by 1.90% with a relative change in radius ΔR of 2.30%. A table with the results for the the increase in power-capture (ΔP) and radius (ΔR) for 4 designs ($R_{exp} = 2, 3, 5, 6$) can be seen in figure 6. As a In conclusion, rotors with an active static aerodynamic DDLC should not be designed for maximum C_P as more power can be generated by rotors with lower C_T and a larger radius R, without violating the relevant DDLC. The changes in loading is explained in the next section.

Effect on loads

Even though meeting the constraint limits means that the chosen DDL will be the same as the baseline, it is interesting to know what happens to the loads that scale different differently than the DDL. As an example, if the DDLC is M_{flap} ($R_{exp} = 3$) it is given that it will not change relative to the baseline, but it could be interesting to know what happens to the T and δ_{tip}.
To investigate it we will introduce a *Generalized Load* (L) as a measure of how loads a load scale.

$$L = K_0 V_0^2 C_T R^{L_{exp}} \tag{39}$$

Where K_0 is a scaling constant and L_{exp} is the *Generalized Load Exponent*. The Generalized Load equation can be made non-dimensional as:

$$\tilde{L} = \frac{L}{K_0 V_0^2 R_0^{L_{exp}}} = C_T \tilde{R}^{L_{exp}} \tag{40}$$

The difference between L_{exp} and R_{exp} is that R_{exp} results in a design, wheres L_{exp} is a load for a design. As an example take a design made for tip-deflection ($R_{exp} = 5$) then $L_{exp} = 3$ will describe the M_{flap} load for that design.
An equation for the relative change $\Delta\tilde{L}$ can be found in terms of the baseline rotor as:

$$\left.\begin{aligned} \tilde{L} &= C_T \tilde{R}^{L_{exp}} \quad (40) \\ \tilde{R} &= \left(\frac{C_{T,0}}{C_T}\right)^{\frac{1}{R_{exp}}} \quad (30) \\ \tilde{L}_0 &= C_{T,0}\tilde{R}_0^{L_{exp}} = C_{T,0} \end{aligned}\right\} \implies \Delta\tilde{L} = \frac{\tilde{L}}{\tilde{L}_0} - 1 = \left(\frac{C_T}{C_{T,0}}\right)^{1-\frac{L_{exp}}{R_{exp}}} - 1 \tag{41}$$

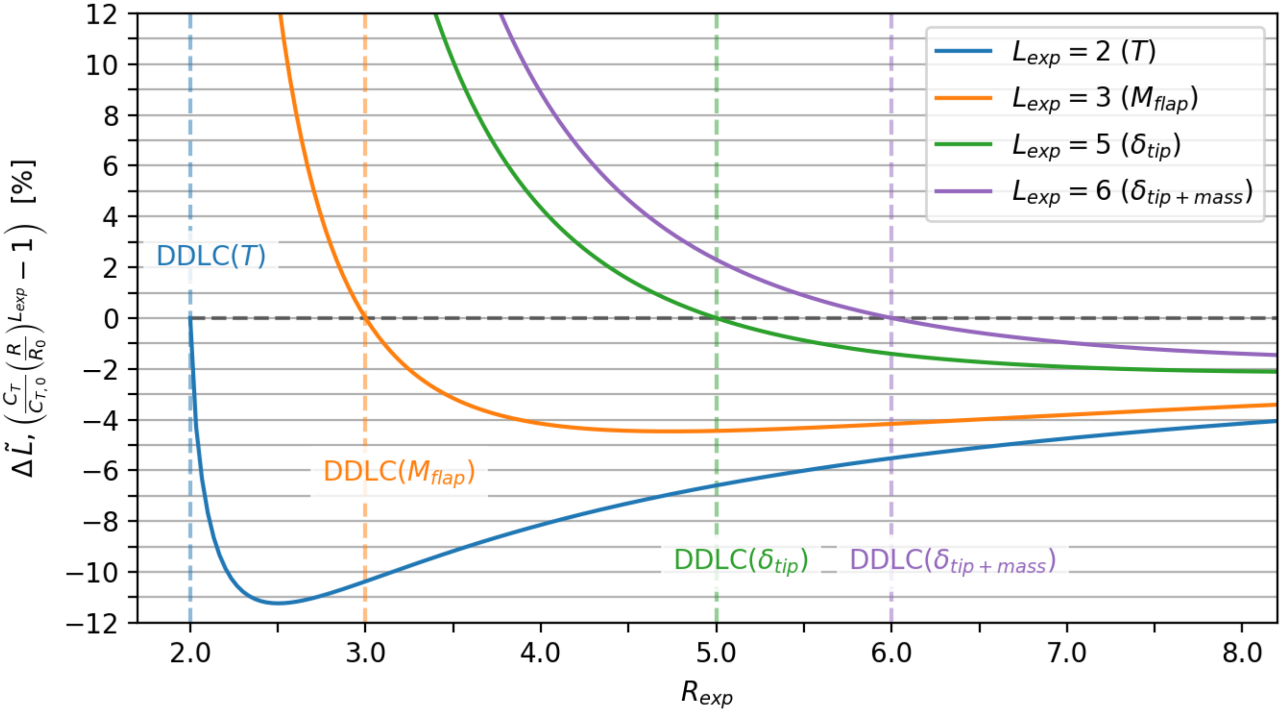

Figure 5. Relative change in different rotor load parameters ($\Delta\tilde{L}$) depending on DDLC. The scaling of loads have the form $\tilde{L} = C_T R^{L_{exp}}$, e.g. $L_{exp} = 2$ scales as the rotor thrust T and $L_{exp} = 5$ scales as the tip deflection δ_{tip}. Each curve depicts how a load parameter would change depending on design driving constraint. As an example consider a design limited by tip deflection DDLC(δ_{tip}), i.e. $R_{exp} = 5$ matching the dashed green line. Tip deflection meets requirements, while thrust (T) is lowered 6.6% and flap moment M_{flap} by 4.4%.

Since it is known that $C_T \leq C_{T,0}$ the following can be concluded:

$L_{exp} < R_{exp}$	The load is lower than the baseline level
$L_{exp} = R_{exp}$	The load is identical to the baseline level
$L_{exp} > R_{exp}$	The load is larger than the baseline level

This agrees with figure 5, which illustrates the effect of design constraints (DDLC) on different loads. For example, consider tip-deflection ($R_{exp} = 5$, DDLC(δ_{tip}), dashed green line). Looking at the green solid line ($L_{exp} = 5$) it is seen that the relative change in L is zero as expected. Now looking at the loads with $L_{exp} < R_{exp}$, namely thrust ($L_{exp} = 2$) and flap-moment ($L_{exp} = 3$) it is seen that ΔL is lower than the baseline with $\Delta T = -6.6\%$ and $\Delta M_{flap} = -4.4\%$. But the loads where $L_{exp} > R_{exp}$ the loads are increased. If there was a load that scaled like $L_{exp} = 6$ the load would be increased by $\Delta L_{(L_{exp}=8)} = +2.3\%$$\Delta L_{(L_{exp}=6)} = +2.3\%$. Furthermore, figure 5 shows that the relative decrease in load is always most pronounced for the thrust ($L_{exp} = 2$), the biggest impact occurring around $R_{exp} \approx 2.5$. All the relative change curves have distinct minima, but at the same time are characterized by large plateaus of relatively small change. Another observation is how quickly the curves grows for $L_{exp} > R_{exp}$. As an example take DDLC(M_{flap}) in this case $\Delta\delta_{tip} = +24.5\%$ and $\Delta L_{(L_{exp}=6)} = +38.9\%$. The relative change in loads becomes smaller as R_{exp} increases. A sketch with a zoomed view of the tip and a table with the values can be seen in figure 6.

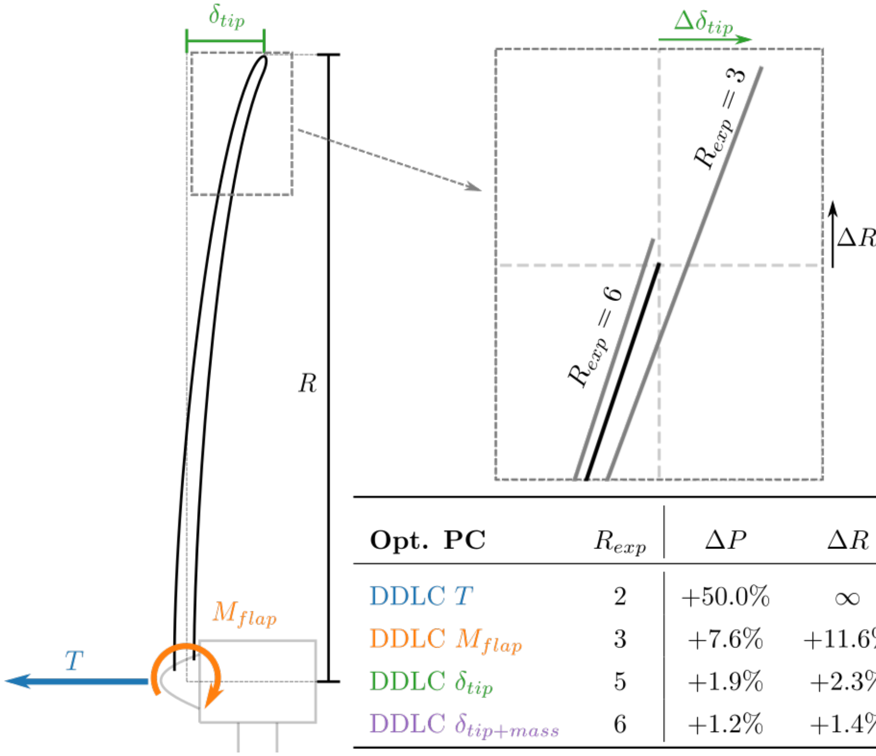

Opt. PC	R_{exp}	ΔP	ΔR	$(L_{exp}=2)$ ΔT	$(L_{exp}=3)$ ΔM_{flap}	$(L_{exp}=5)$ $\Delta\delta_{tip}$
DDLC T	2	+50.0%	∞	**0.0%**	∞	∞
DDLC M_{flap}	3	+7.6%	+11.6%	-10.4%	**0.0%**	+24.5%
DDLC δ_{tip}	5	+1.9%	+2.3%	-6.6%	-4.4%	**0.0%**
DDLC $\delta_{tip+mass}$	6	+1.2%	+1.4%	-5.5%	-4.2%	-1.4%

Figure 6. Sketch of a turbine with the load/structural response outlined. The zoomed figure shows the radius increase (ΔR) and the change in tip-deflection ($\Delta\delta_{tip}$) for two different DDLCs (bold black line is the baseline). The table shows the relative change in power, radius and load/structural response for different DDLCs. $R_{exp} = 2$ is a thrust constraint design, $R_{exp} = 3$ is a flap moment constraint design, $R_{exp} = 5$ is a tip-deflection constraint design and $R_{exp} = 6$ is tip-deflection+constant mass constraint design.

4.2 ~~Low induction rotor~~Low-Induction-Rotor

The concept was mentioned in the introduction since it has had some attention over the recent years. The ~~Low Induction Rotors~~ Low-Induction-Rotors (LIR) are rotors designed with lower axial induction a than the level that maximizes C_P. The concept is to a certain degree analogous with optimization of rotors ~~with respect to~~ for power-capture. ~~Using the value for C_T from~~

To investigate such an LIR design it is chosen to fix the C_T value below rated power to be the same as for the power-capture optimization ~~will not give the a design that will reach~~ for a given R_{exp}. If the radius was set to the same value as for power-capture it will result in the constraint limit ~~, since the increase in rotor radius will make the turbine reach~~ not being met since the turbine reaches rated power earlier~~than the baseline. An additional optimization is therefore required where R is increase until~~ . Since C_T is fixed and the constraint limit ~~is reached.~~needs to be met, then the wind speed at which the turbine reaches rated power ($\tilde{V}_{rated}$) can be found. It is found through the normalized power (the integrant of equation 7 without the PDF_{wind}) and the constraint limit with wind speed scaling (equation 30 multiplied with $\tilde{V}^2$):

$$\left.\begin{array}{c} \frac{27}{16}\frac{1}{2}\left(1+\sqrt{1-C_T}\right)C_T\tilde{R}^2\tilde{V}^3=1 \\ \tilde{V}^2\frac{C_T}{C_{T,0}}\tilde{R}^{R_{exp}}=1 \end{array}\right\} \implies \tilde{V}_{rated}=\left(\frac{16}{27}\frac{2}{\left(1+\sqrt{1-C_T}\right)C_T}\left(\frac{C_T}{C_{T,0}}\right)^{\frac{2}{R_{exp}}}\right)^{\frac{1}{3-\frac{4}{R_{exp}}}} \quad (42)$$

With the rated wind speed the rotor radius can be found using the following steps:

1) $C_T=\frac{8\left(R_{exp}^2-3R_{exp}+2\right)}{(3R_{exp}-4)^2}$ (38)

2) $\tilde{V}_{rated}=\left(\frac{16}{27}\frac{2}{\left(1+\sqrt{1-C_T}\right)C_T}\left(\frac{C_T}{C_{T,0}}\right)^{\frac{2}{R_{exp}}}\right)^{\frac{1}{3-\frac{4}{R_{exp}}}}$ (42)

3) $\tilde{R}=\left(\frac{1}{\tilde{V}_{rated}^2}\frac{C_{T,0}}{C_T}\right)^{\frac{1}{R_{exp}}}$ (43)

With C_T, $\tilde{V}_{rated}$ and $\tilde{R}$, $A\tilde{E}P$ can be computed using equation 7.

The LIR is illustrated by the examples in figure 7 and 8 where the present ~~design~~ analysis framework has been applied with constraints pertaining to respectively flap moments ($R_{exp}=3$) and tip deflections ($R_{exp}=5$).

In both cases, the resulting power curves are slightly above the equivalent baseline ones, and the thrust peaks are reduced compared with the baseline. The relative change in AEP results in a smaller change than the change in power at the design point. For the case with DDLC(M_{flap}), $\Delta AEP=6.0\%$ while the ~~power capture~~ power-capture increased by $\Delta P=7.6\%$. The corresponding improvements for a tip deflection constrained rotor (DDLC(δ_{tip})) are ~~$\Delta AEP=1.1\%$~~ $\Delta AEP=1.2\%$ and $\Delta P=1.9\%$. The lower relative improvement for the LIR is related to the amount of the power that is produced below rated power. The results for LIR ~~is~~ are summarized in figure 9 with a table and a sketch showing the relative changes in AEP, radius, thrust, root-flap-moment and tip-deflection for 4 different designs ($R_{exp}=2,3,5,6$). From figure 9 the thrust constraint design (DDLC, T; $R_{exp}=2$) is seen to have diverging values for ΔR, ΔM_{flap} and $\Delta\delta_{tip}$. As it was the case for power-capture optimization these results are found from investigating the result in the limit where $R_{exp}\to 2$. Even though this result of $\Delta R\to\infty$ is interesting, the corresponding consequence of $\Delta M_{flap}\to\infty$ makes this infeasible for practical use, so this will not be studied further here.

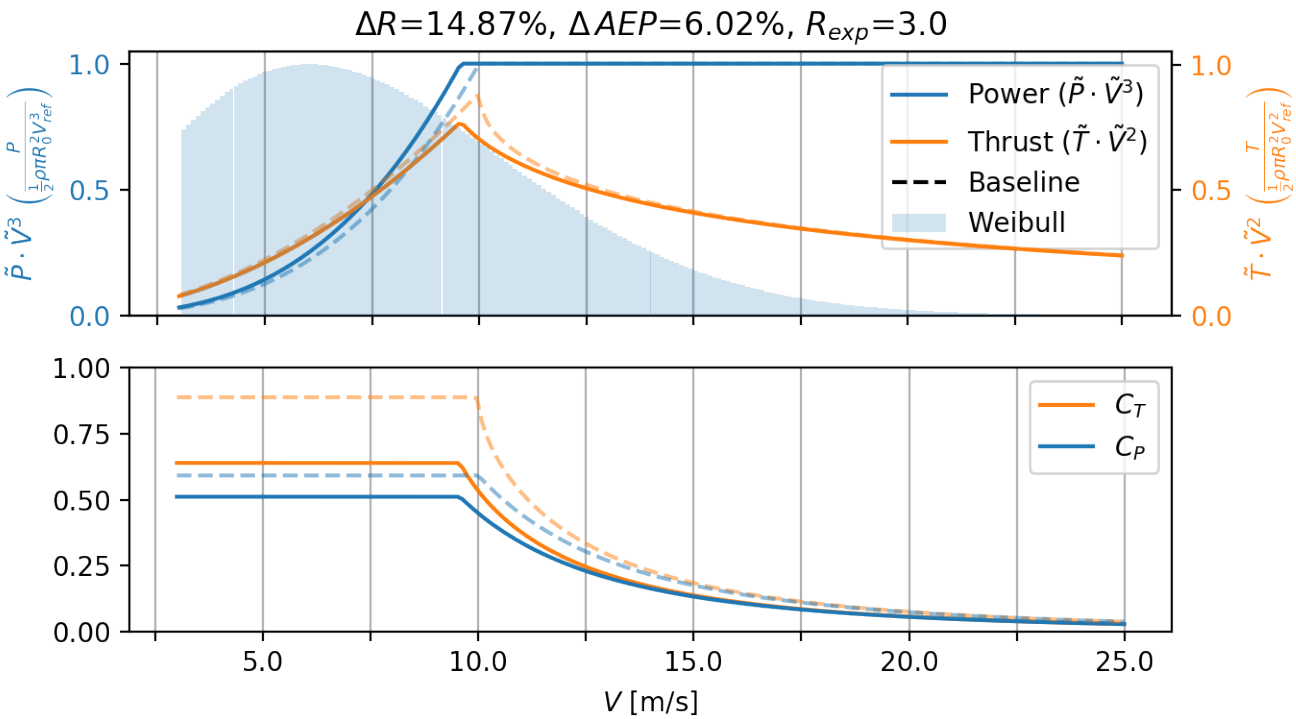

Figure 7. Power and thrust curves for ~~low induction rotor~~Low-Induction-Rotor (solid lines), designed using the present method with DDLC exponent $R_{exp} = 3$, which corresponds to a M_{flap} constraint. The dashed line is the baseline rotor optimized for max C_P.

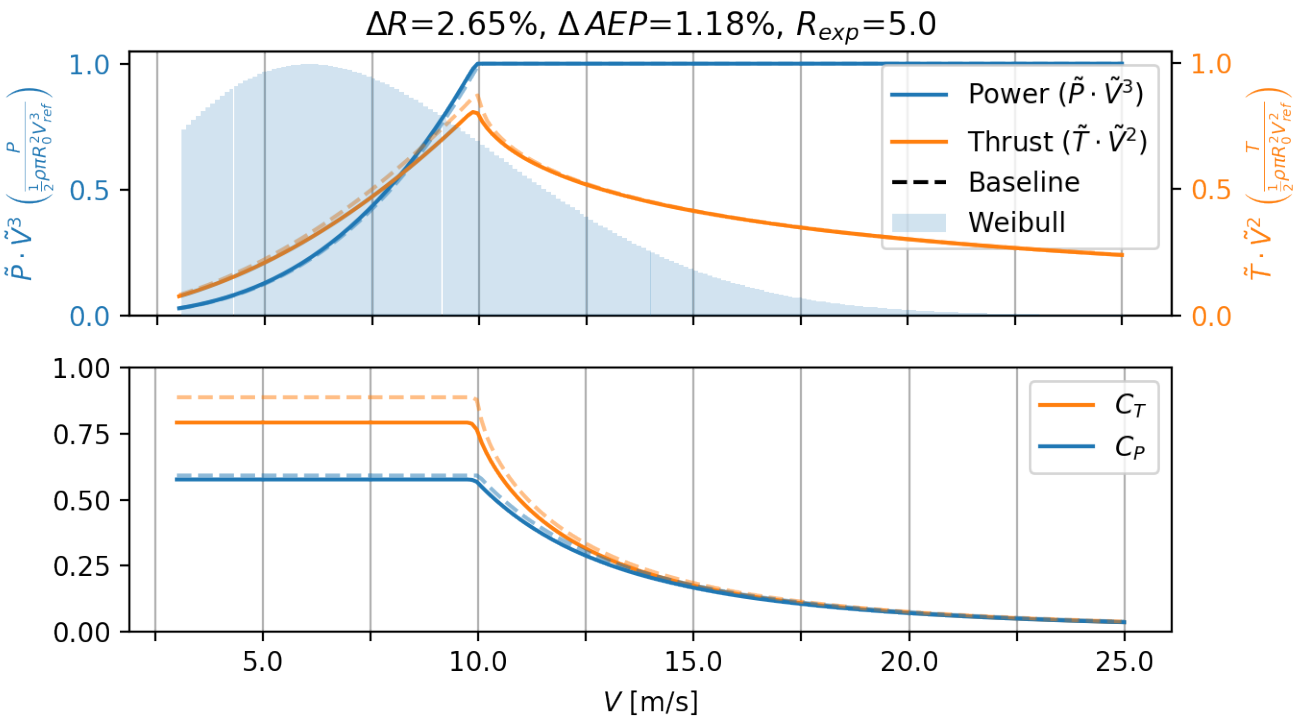

Figure 8. Power and thrust curves for rotor with DDLC exponent $R_{exp} = 5$ (solid lines), corresponding to a δ_{tip} constraint. The dashed line is the baseline rotor optimized for max C_P.

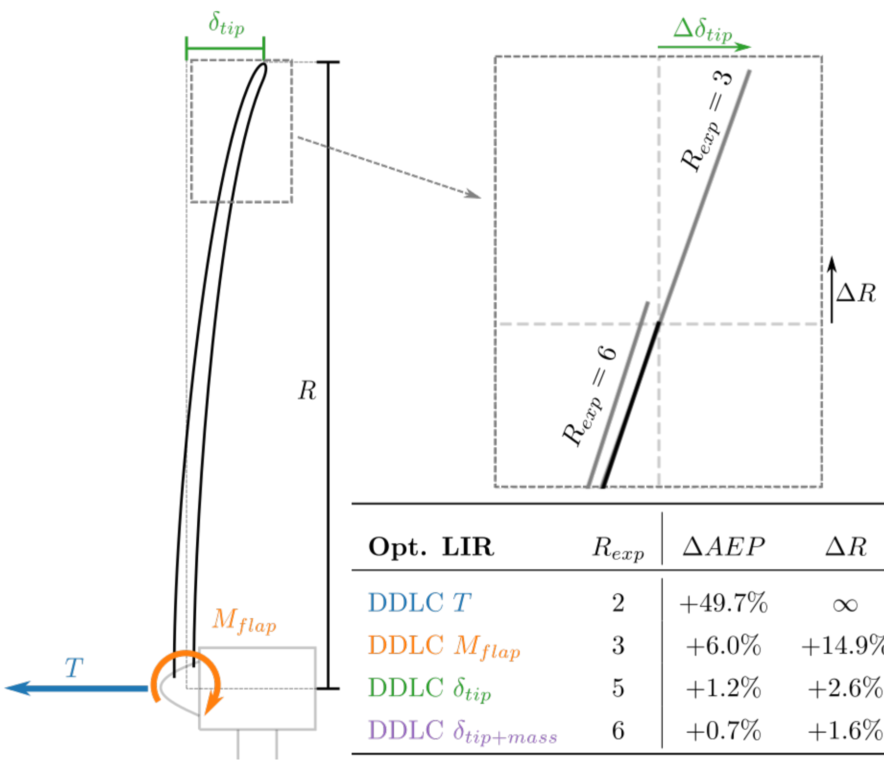

Opt. LIR	R_{exp}	ΔAEP	ΔR	(L_{exp}=2) ΔT	(L_{exp}=3) ΔM_{flap}	(L_{exp}=5) $\Delta\delta_{tip}$
DDLC T	2	+49.7%	∞	**0.0%**	∞	∞
DDLC M_{flap}	3	+6.0%	+14.9%	-12.9%	**0.0%**	+31.9%
DDLC δ_{tip}	5	+1.2%	+2.6%	-7.5%	-5.1%	**0.0%**
DDLC $\delta_{tip+mass}$	6	+0.7%	+1.6%	-6.2%	-4.7%	-1.6%

Figure 9. Sketch of a turbine with the load/structural response outlined. The zoomed figure shows the radius increase (ΔR) and the change in tip-deflection ($\Delta\delta_{tip}$) for two different DDLCs (bold black line is the baseline). The table shows the relative change in power, radius and load/structural response for different DDLCs. $R_{exp} = 2$ is a thrust constraint design, $R_{exp} = 3$ is a flap moment constraint design, $R_{exp} = 5$ is a tip-deflection constraint design and $R_{exp} = 6$ is tip-deflection+constant mass constraint design.

4.3 AEP optimized rotor

As mentioned in section 3, the variables considered for optimization of AEP are $C_T(\tilde{V})$ as well as $\tilde{R}$. In this formulation, C_T can be adjusted independently for each wind speed, which ideally can be achieved through blade pitch control. The relative radius $\tilde{R}$ couples the rotor operation across all wind speeds, as it necessarily is constant. Based on initial studies, the optimizer targets solutions with three distinct operational ranges, which ordered by wind speed are:

- Operation with maximum power ~~efficiency~~ coefficient (max C_P)
- Operation at constraint limit (constant thrust T)
- Operation at rated power

this can be used to make C_T a function of $\tilde{R}$ hereby decreasing the optimization problem to an unconstrained optimization in one variable ($\tilde{R}$). The C_T function is given as:

$$C_T(\tilde{V},\tilde{R}) = \begin{cases} \frac{8}{9} & \frac{8}{9} \leq \tilde{V}^{-2} C_{T,0} \tilde{R}^{-R_{exp}} & (\max\ C_P) \\ \tilde{V}^{-2} C_{T,0} \tilde{R}^{-R_{exp}} & 1 \leq \frac{27}{16}\frac{1}{2}\left(1+\sqrt{1-C_T}\right) C_T \tilde{R}^2 \tilde{V}^3 & \text{(constraint limit)} \\ 1 = \frac{27}{16}\frac{1}{2}\left(1+\sqrt{1-C_T}\right) C_T \tilde{R}^2 \tilde{V}^3 & 1 > \frac{27}{16}\frac{1}{2}\left(1+\sqrt{1-C_T}\right) C_T \tilde{R}^2 \tilde{V}^3 & \text{(rated power)} \end{cases} \quad (44)$$

Where the last equation needs to be solved to get C_T, the solution is a third-order polynomial, which is easier solved numerically.

The only free parameter that ~~need~~ needs to be determined to find the optimal AEP is $\tilde{R}$. The optimization problem can ~~therefore~~ be reformulated as:

$$\underset{\tilde{R}}{\text{maximize}} \quad A\tilde{E}P = \int_{\tilde{V}_{CI}}^{\tilde{V}_{CO}} \tilde{P}(C_T(\tilde{V},\tilde{R}),\tilde{R}) \cdot \tilde{V}^3 \cdot PDF_{wind}(\tilde{V}) d\tilde{V} \quad (45)$$

The problem can be solved with most optimization solvers since the AEP can be computed explicitly if $\tilde{R}$ is given. The optimization problem was solved with the L-BFGS-B algorithm described in Zhu et al. (1997) though the use of Scipy (Millman and Aivazis (2011)).

Examples of the resultant power and thrust curves can be seen in figure 10 and 11, for DDLC(M_{flap}) and DDLC(δ_{tip}) respectively. Looking at figure 10 ($R_{exp} = 3$) it is clear that the power and thrust curves ~~has~~ have changed quite substantially, compared to the baseline Betz-rotor (dashed curves). The thrust curve ~~do~~ does not have a sharp peak ~~any more~~anymore, but a flat plateau. ~~This is often refereed~~ As mentioned in the introduction this is often referred to as thrust-clipping~~, peak-shaving or force-capping~~. It comes from the DDLC equation 44 which shows that $C_T \propto \tilde{V}^{-2}$, and since thrust is proportional to $T \propto C_T \tilde{V}^2$ it means that the thrust is constant. As mentioned, the region where the rotor is ~~thrust-cliped~~ thrust-clipped is also where the DDLC is active, so opposed to the baseline and LIR rotor the DDLC is active over a larger range of V. The larger range of V is also part of why $\Delta R = 44.6\%$ which is a huge increase. As a result, it also leads to a large increase in

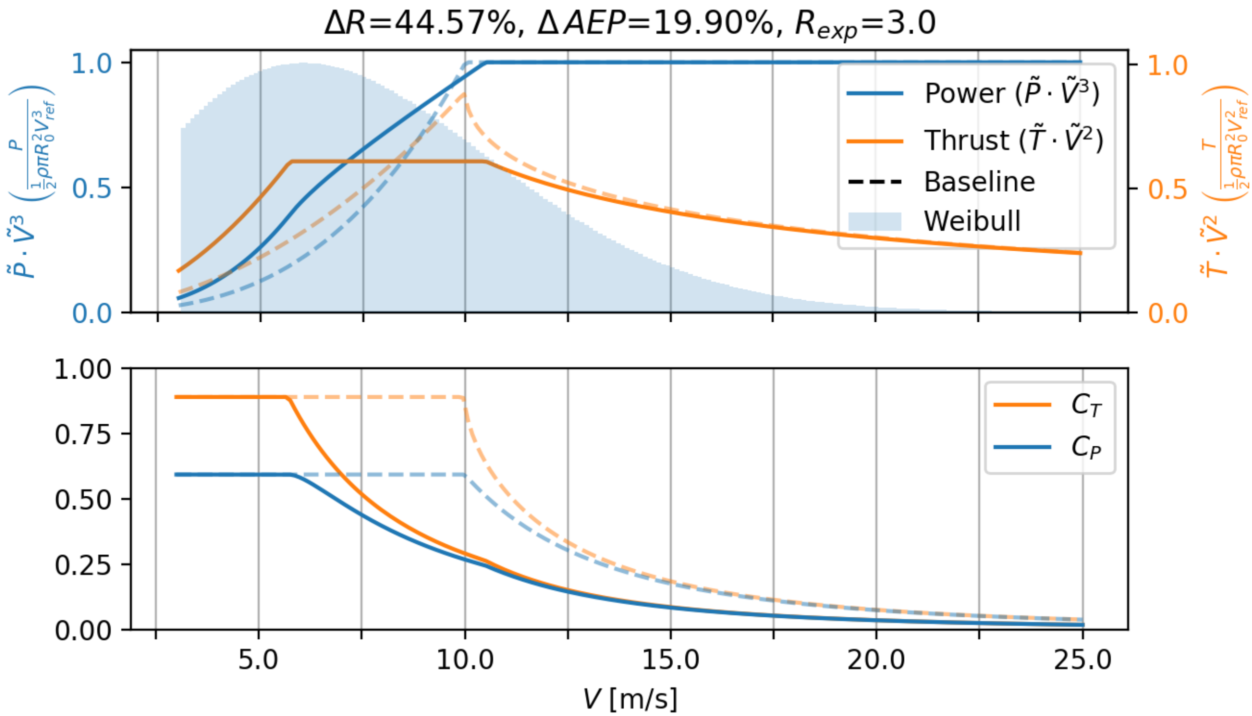

Figure 10. Power and thrust curve for AEP optimized rotor (solid lines) with DDLC exponent is $R_{exp} = 3$ which is equivalent to a constraint on M_{flap}. The dashed line is the baseline rotor optimized for max C_P below rated power.

$\Delta AEP = 19.9\%$. This is a very large change in $\tilde{R}$ and the feasibility of such a design is doubtful. As it is shown later the change in maximum loads (see figure 13) shows a significant change in loads with $L_{exp} > R_{exp}$.

A more realistic design for modern turbines is found in figure 11 ($R_{exp} = 5$). Here the changes ~~is~~ are less but still significant with $\Delta R = 10.7\%$ and $\Delta AEP = 5.8\%$. It shows the same shape with the ~~thrust-cliped~~ thrust-clipped curve, but now it is over a smaller range of V. ~~Thrust-clipping~~ As mentioned in the introduction thrust-clipping is also found by Buck and Garvey (2015a) to be a beneficial way to lower CoE.

In figure 12 the relative change in R and AEP can be see as a function of the DDLC R-exponent. The plot both contains the result for the AEP-optimized rotor (AEP opt.~~,~~ ; solid black line) and ~~for the Low Induction Rotor (Low ind.~~ the Low-Induction-Rotor (LIR opt.; dash-dotted gray line). The difference between the two is significant especially for ΔAEP. ~~A thing to notes is that in both cases ΔR grows to infinity as R_{exp} goes toward 2. But for ΔAEP it will go towards a finite value.~~ The results for the AEP optimized rotor ~~is~~ are summarized in figure 14 with a table and a sketch, that shows the relative changes~~in radius. The loads are explained in the next section~~. As it was the case for power-capture optimization and LIR optimization some values diverge when $R_{exp} \to 2$ and the results are found by investigating this limit. But since it has no practical value, further explanation is omitted here.

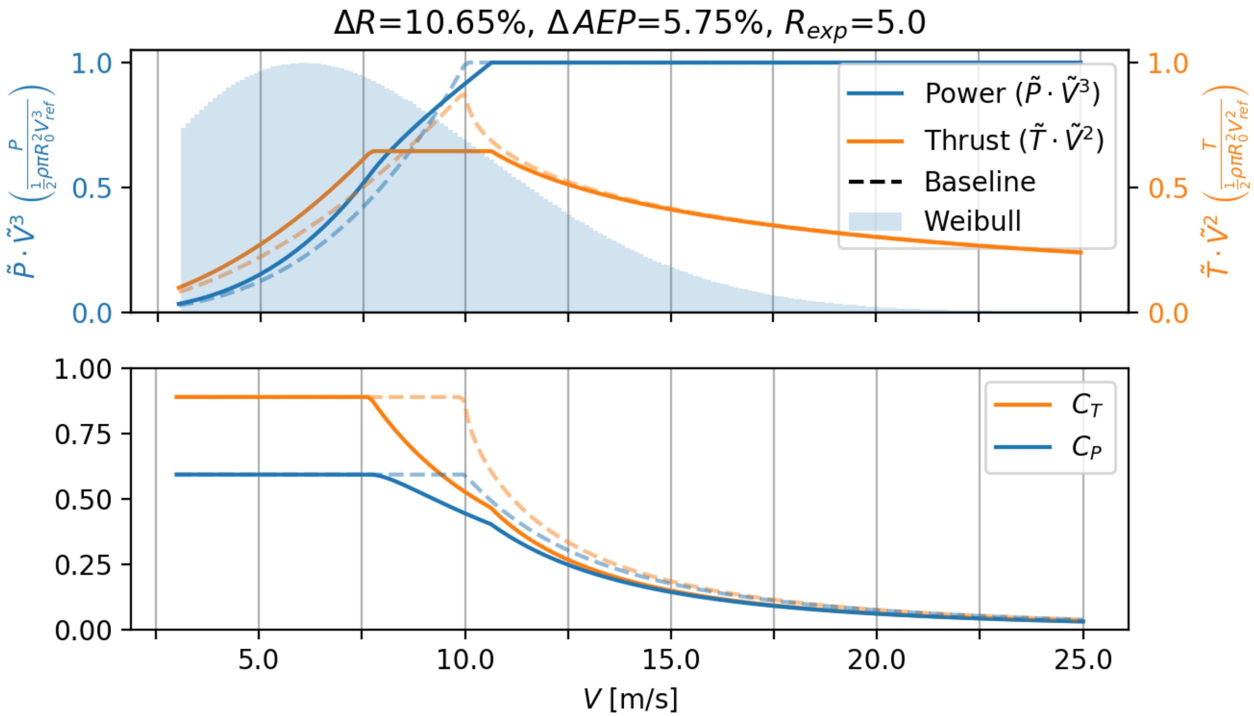

Figure 11. Power and thrust curve for AEP optimized rotor (solid lines) with DDLC exponent is $R_{exp} = 5$ which is equivalent to a constraint on δ_{tip}. The dashed line is the baseline rotor optimized for max C_P below rated power.

Effect on loads

In figure 13 a plot of the relative change in maximum loads as a function of the DDLC R-exponent. The relative max load ($\Delta\tilde{L}_{\max}$) is not comparing the loads at each $\tilde{V}$ but the max load for the baseline at $\tilde{V} = 1$ (rated wind speed) to the max load for the optimized rotor for any $\tilde{V}$. The plot in figure 13 is similar to the plot in figure 5 with the difference being that it is ~~for the AEP-optimized rotor and Power-Capture optimized rotor respectively~~the relative change in maximum loads, independently of wind speed at which it occurred. Comparing the two plots, one should note the range for the y-scale in the two plots~~should be noted~~, with figure 13 having the larger range. It also means that the relative change in the loads for the AEP-optimized rotor experiencing a larger relative change. But it also has the consequence that loads with $L_{exp} > R_{exp}$ grows faster especially for larger values of R_{exp} (> 5). A summary for the AEP optimized rotor can be seen in figure 14, where a table for 4 different design ($R_{exp} = 2, 3, 5, 6$) shows the relative change in AEP, radius, thrust, root-flap-moment and tip-deflection.

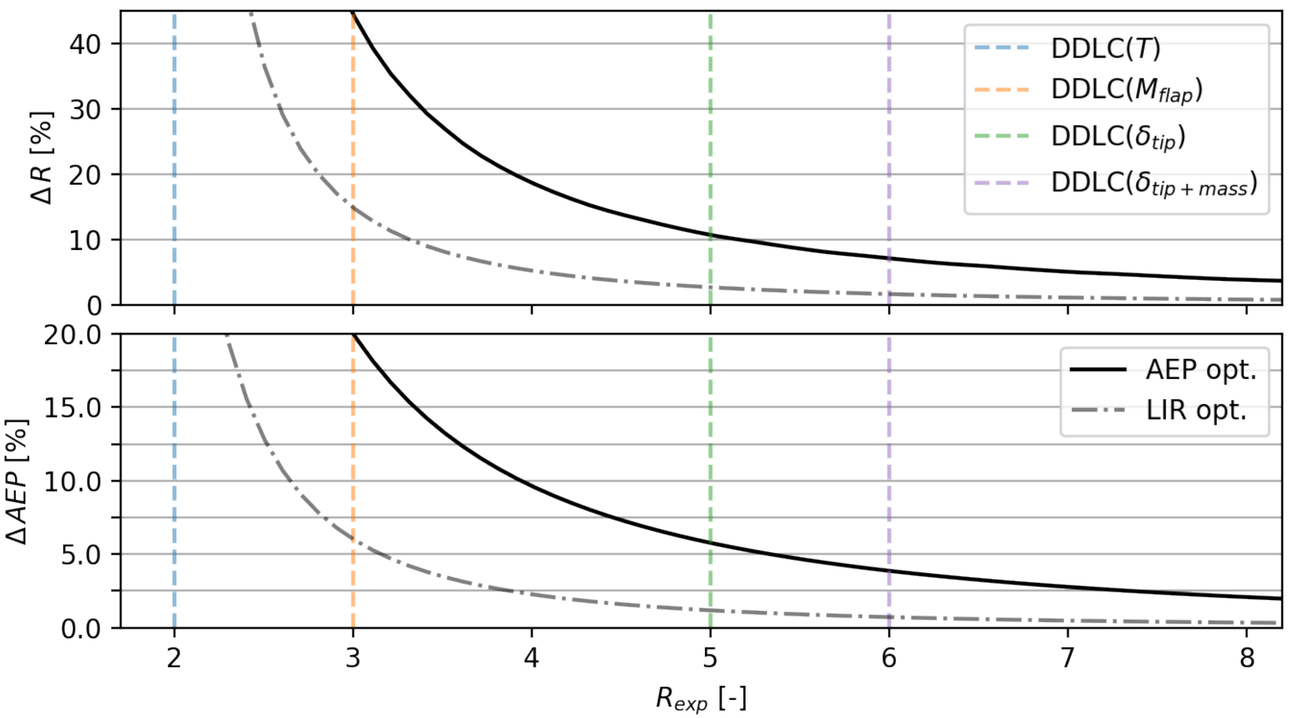

Figure 12. DDLC exponent (R_{exp}) vs. relative change in radius (upper graph, ΔR) and relative change in AEP (lower graph, $\Delta A\tilde{E}P$). The plot both contains the changes for the case for ~~Low Induction~~ Low-Induction-Rotor (~~Low Ind~~LIR opt., black dashed-dot) and the AEP optimized (AEP opt., black solid). The changes in both AEP and radius is much larger for the AEP optimized rotor.~~It should be noted that in both cases ΔAEP has a finite value as $R_{exp} \to 2$, but ΔR is approaching infinity.~~

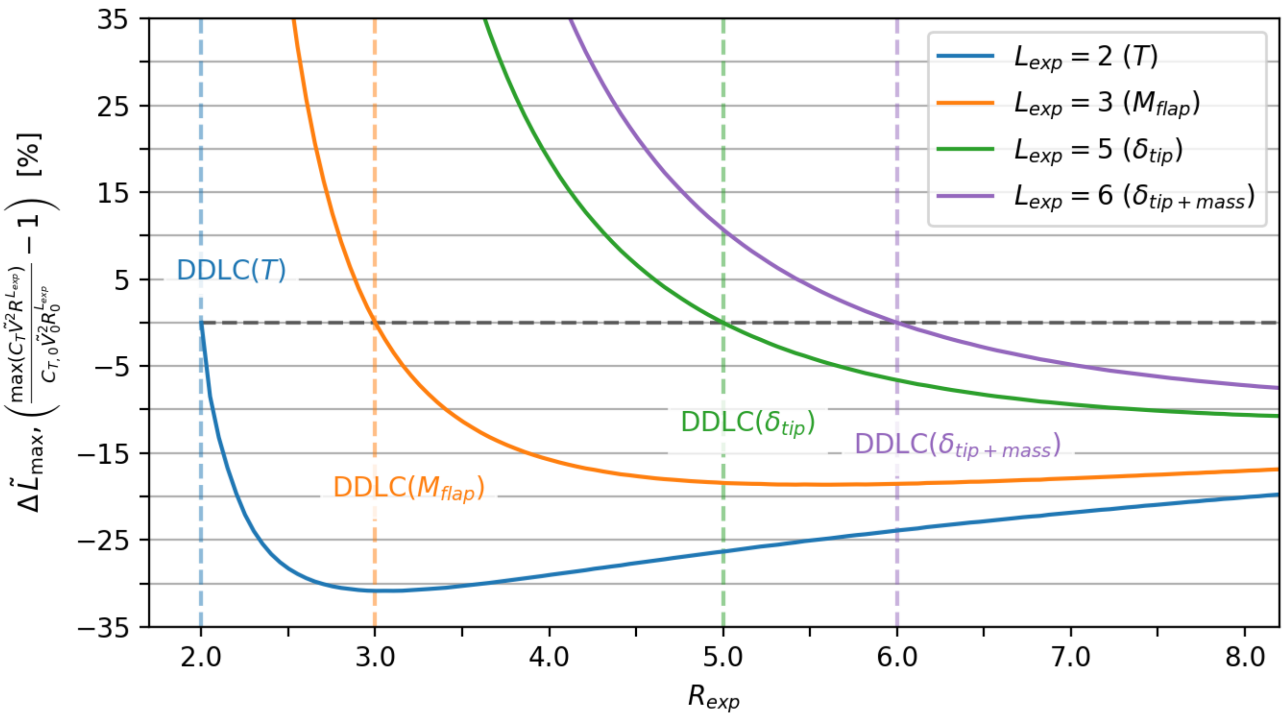

Figure 13. DDLC R-exponent (R_{exp}) vs. relative maximum load ($\Delta\tilde{L}_{\max}$). ~~It is a similar~~ The plot looks similar to figure 5 but ~~here it~~ $\Delta\tilde{L}_{\max}$ is ~~for~~ the ~~AEP-optimized rotor and~~ change in maximum loading. As an example, when thrust (T) is -30.8% for $R_{exp} = 3$ it means that the maximum thrust (for any wind speed) is 30.8% lower than the ~~change in~~ maximum thrust for the ~~max load~~baseline (which happens just before rated wind speed). ~~The~~ Notice that the range for the y-scale is much larger it this plot than for the power-capture optimized rotor. The potential reduction is ~~therefore~~ more, but it comes with the consequence that $L_{exp} > R_{exp}$ grows faster even for high values of R_{exp}

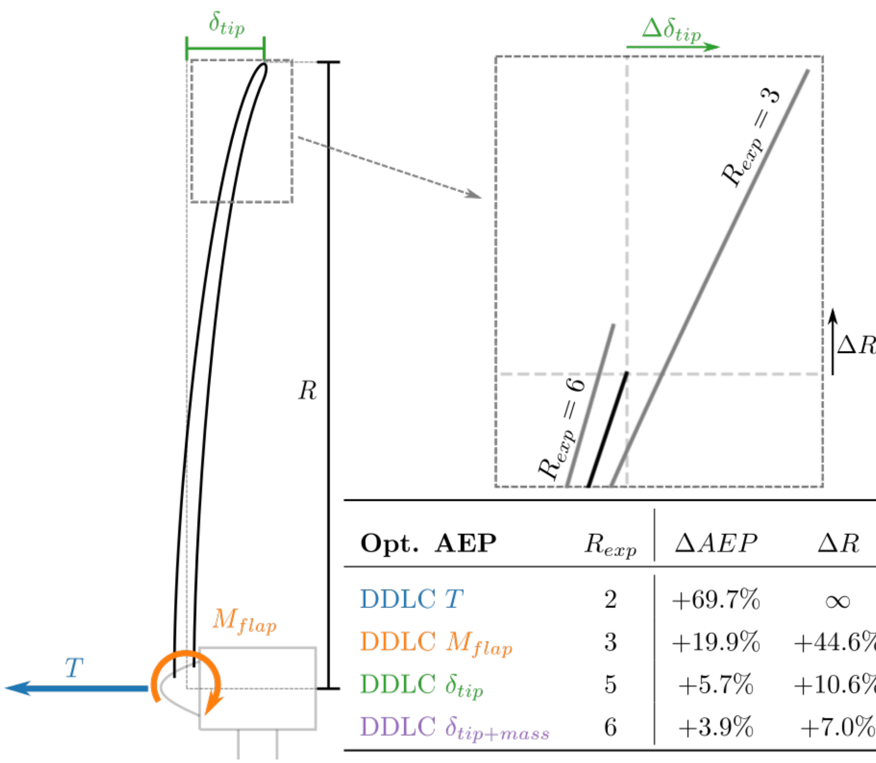

Opt. AEP	R_{exp}	ΔAEP	ΔR	(L_{exp}=2) ΔT	(L_{exp}=3) ΔM_{flap}	(L_{exp}=5) $\Delta\delta_{tip}$
DDLC T	2	+69.7%	∞	**0.0%**	∞	∞
DDLC M_{flap}	3	+19.9%	+44.6%	-30.8%	**0.0%**	+109.0%
DDLC δ_{tip}	5	+5.7%	+10.6%	-26.2%	-18.3%	**0.0%**
DDLC $\delta_{tip+mass}$	6	+3.9%	+7.0%	-23.8%	-18.4%	-6.6%

Figure 14. Sketch of a turbine with the load/structural response outlined. The zoomed figure shows the radius increase (ΔR) and the change in tip-deflection ($\Delta\delta_{tip}$) for two different DDLCs (bold black line is the baseline). The table shows the relative change in power, radius and load/structural response for different DDLCs. $R_{exp} = 2$ is a thrust constraint design, $R_{exp} = 3$ is a flap moment constraint design, $R_{exp} = 5$ is a tip-deflection constraint design and $R_{exp} = 6$ is tip-deflection+constant mass constraint design.

4.4 Summary of Findings

In table 1 the tables shown in the figures 6,9 and 14 is summarized. It compares the different optimization's to each other.

Opt. PC	R_{exp}	ΔP	ΔR	$(L_{exp}=2)$ ΔT	$(L_{exp}=3)$ ΔM_{flap}	$(L_{exp}=5)$ $\Delta\delta_{tip}$
DDLC T	2	+50.0%	∞	**0.0%**	∞	∞
DDLC M_{flap}	3	+7.6%	+11.6%	-10.4%	**0.0%**	+24.5%
DDLC δ_{tip}	5	+1.9%	+2.3%	-6.6%	-4.4%	**0.0%**
DDLC $\delta_{tip+mass}$	6	+1.2%	+1.4%	-5.5%	-4.2%	-1.4%

Opt. LIR	R_{exp}	ΔAEP	ΔR	$(L_{exp}=2)$ ΔT	$(L_{exp}=3)$ ΔM_{flap}	$(L_{exp}=5)$ $\Delta\delta_{tip}$
DDLC T	2	+49.7%	∞	**0.0%**	∞	∞
DDLC M_{flap}	3	+6.0%	+14.9%	-12.9%	**0.0%**	+31.9%
DDLC δ_{tip}	5	+1.2%	+2.6%	-7.5%	-5.1%	**0.0%**
DDLC $\delta_{tip+mass}$	6	+0.7%	+1.6%	-6.2%	-4.7%	-1.6%

Opt. AEP	R_{exp}	ΔAEP	ΔR	$(L_{exp}=2)$ ΔT	$(L_{exp}=3)$ ΔM_{flap}	$(L_{exp}=5)$ $\Delta\delta_{tip}$
DDLC T	2	+69.7%	∞	**0.0%**	∞	∞
DDLC M_{flap}	3	+19.9%	+44.6%	-30.8%	**0.0%**	+109.0%
DDLC δ_{tip}	5	+5.7%	+10.6%	-26.2%	-18.3%	**0.0%**
DDLC $\delta_{tip+mass}$	6	+3.9%	+7.0%	-23.8%	-18.4%	-6.6%

Table 1. Overview of the optimization results from optimizing Power-Capture (Opt. PC), Low-Induction-Rotor (Opt. LIR) and Annual Energy Production (Opt. AEP)

As seen from the tables the largest increase in $\Delta P/AEP$ is found using AEP-optimization, which also leads to the largest increase in rotor radius (ΔR). It also shows that using thrust-clipping seems to be a better operational strategy than low-induction, as the design driving constraint can be met over a larger range of wind speeds and low-induction is only needed around maximum thrust and not at low wind speeds.

In all three optimization cases, the optimization of the design with thrust constraint (DDLC. T; $R_{exp} = 2$) leads to divergent values for ΔR and the loads. In all cases the result are found though investigating the limit value behavior when $R_{exp} \to 2$. Since this is not thought to be of much practical value, the details are not provided here.

4.5 Limitation of the study and possible improvements

The study shows that for a rotor constraint by a static aerodynamic DDL there is a benefit in lowering the loading and increasing the rotor size in terms of power/AEP. But as it was found by Bottasso et al. (2015) having a rotor with the same load constraint and increasing the radius does not mean that the cost is the same or that it is ~~cost optimal~~cost-optimal. They found that the increase in AEP did not compensate for the added cost by increasing the rotor radius. This problem of the ~~cost benefit~~ cost-benefit is not directly addressed in this paper ~~,~~ but by the DDLC $\delta_{tip+mass}$ a constraint where the mass is kept constant. It is thought to be a better approximation for a rotor with a fixed price - but this assumption needs to be tested.

Another issue that is not taken into account in this study is the influence of the turbines "~~self weight~~self-weight". As ~~it~~ was found by Sieros et al. (2012) the ~~self weight~~ self-weight becomes more important for larger rotors. ~~In order to~~ To accommodate for the added mass, a penalty could be added which should scale as $\tilde{R}$ or $\tilde{R}^3$ for "top head mass" and "static blade mass moment" respectively. As discussed above there could also be implemented a constraint that will keep the mass or the mass moment. Again this is a limitation of the study.

The fidelity of the models is also a limitation. Even though 1D-aerodynamic-momentum theory is a common approximation to do for ~~first order~~ first-order studies in rotor design it is well known that the constantly loaded rotor is not possible to realize and when losses are included the ~~constant~~ constantly loaded rotor is not the optimal solution ~~any more~~anymore. At the same time if it was possible to decrease the load at the tip more than at the root it would lead to less tip-deflection than a ~~constant~~ constantly loaded rotor with a similar C_T. Extending the model to be able to handle radial load distribution is one way of detailing the model that could lead to even larger improvements. It could be done through the use of Blade Element Momentum (BEM) theory.

For modern turbine design, it is often the case that the structural design is determined by the aero-elastic extreme loads, ~~and with~~ such as extreme turbulence or gusts. With the simplicity of the models in this study, this is not taken into consideration. But if the extreme load happens in normal operation ~~it is likely that there is~~ there will likely be a direct relationship between the steady- and extreme loads, meaning that a decrease in steady loads will also ~~will~~ lead to a decrease in the extreme load. This is an assumption that should be tested in future work.

If the design driving load is happening in non-operational conditions, e.g. extreme wind in parked conditions, grid loss, sub-component failure, etc. the analysis tool cannot be directly applied.

5 Conclusions

A ~~first order~~ first-order model framework for ~~the design~~ analysis of wind turbine rotors was developed based on aerodynamic 1D-momentum theory and Euler-Bernoulli-Beam theory. This framework introduces the concept of *Design Driving Load* (DDL) for which a generalized form has been developed where loads only differ by a scaling exponent R_{exp}, e.g. thrust scales as $R_{exp} = 2$, root-flap-moment as $R_{exp} = 3$ and tip-deflection as $R_{exp} = 5$. Despite the simplicity of the model, this study has shown important trends in how to design rotors for maximum ~~power capture~~power-capture. It has been shown that the potential increase in ~~power capture~~ power-capture is very dependent on the relevant constraint, e.g. whether thrust is the constraining load or the more restrictive tip-deflection. Furthermore, it was concluded that the best way to design a rotor for increased power capture power-capture using aero-elastic considerations is not to maximize C_P, but rather to relax C_P and operate at lower loading (lower C_T). How much one should relax C_P depends on the chosen design driving constraint (R_{exp}). The results for optimizing for power capture power-capture are summarized in Table 1 (Opt. PC).

The optimization of power capture power-capture determines the best possible design based on for a given wind speed. By considering the *Annual Energy Production* (AEP), an optimal design across the range of operational wind speeds can be found for a given wind speed frequency distribution. Optimal AEP was considered with two different approaches, namely *Low Induction Rotor* *Low-Induction-Rotor* (LIR) and full AEP-optimization. For LIR, the C_T value below rated power was set to the value found from power-capture optimization with respect to for the chosen R_{exp}. Then the radius was increased to maximize AEP while observing the constraint limit compared to the power-capture optimized rotor since it will reach rated power earlier with the same rotor size. A summary of the results can be seen in Table 1 (Opt. LIR).

For the full AEP-optimization, C_T was allowed to take on any positive value below the Betz limit ($0 \leq C_T \leq 8/9$) for all wind speeds. The optimal AEP is obtained for a rotor that operates in three distinct operational regimes:

- Operation with maximum power efficiency coefficient ($\max C_P$)
- Operation at constraint limit (constant thrust T)
- Operation at rated power

The results from the optimization are summarized in Table 1 (Opt. AEP). It shows significantly larger relative improvements in power/energy compared to power-capture and LIR optimized rotors. This comes at the cost of a larger increase in rotor radius. In the range where the optimum turbine operates at the constraint limit, the thrust curve is clipped (also known as peak shaving or force-capping). This is a control feature used for many contemporary turbines, so it is interesting that this study, independently of this knowledge, shows that thrust-clipping is a very efficient way to increase energy capture while observing certain load constraints. It is also the main reason behind the relatively large possible improvements in AEP, as the constraint limit is met over a larger range of wind speeds.

In spite of relatively crude model assumptions made, this paper provides profound insight into the trends of rotor design for maximum power/energy, e.g. the use of thrust clipping. As wind turbine rotors continue to develop towards larger diameters with slender (more flexible) blades, the type of design driving load constraints also evolves. With the present model framework, the conceptual implications of this development become clearer where an increase in AEP of up to 5.7% is possible compared to a traditional C_P optimized rotor - without changing technology, using bend-twist coupling or other advanced features. Finally, this work has demonstrated an approach to formulate an optimization objective that couples power and load/structural response though the power-capture optimization. This approach may be extended into less crude model frameworks, e.g. by introducing radial variations in rotor loading.

Author contributions. KL came up with the concept and main idea, as well as made the analysis. All authors have interpreted the results and made suggestions for improvements. Also, some modeling has changed based on discussions between the authors. KL prepared the paper with revisions of all co-authors.

Competing interests. The authors declare that they have no conflict of interest.

Acknowledgements. We would like to thank Innovation Fund Denmark for funding the industrial PhD project, which this article is a part of.

We would like to thank all employees at Suzlon Blade Sciences Center for being a great source of motivation with their interest in the results.

We would like to thank all people at DTU Risø who came with valuable inputs.

References

Bauchau, O. and Craig, J.: Structural Analysis, https://doi.org/10.1007/978-90-481-2516-6, 2009.

Bottasso, C. L., Campagnolo, F., and Croce, A.: Multi-disciplinary constrained optimization of wind turbines, European Wind Energy Conference and Exhibition 2010, EWEC 2010, 3, 2241–2250, https://doi.org/10.1007/s11044-011-9271-x, 2010.

Bottasso, C. L., Croce, A., and Sartori, L.: Free-form Design of Low Induction Rotors, in: 33rd Wind Energy Symposium, https://doi.org/10.2514/6.2015-0488, 2015.

Buck, J. A. and Garvey, S. D.: Analysis of Force-Capping for Large Wind Turbine Rotors, Wind Engineering, 39, 213–228, https://doi.org/10.1260/0309-524X.39.2.213, 2015a.

Buck, J. A. and Garvey, S. D.: Redefining the design objectives of large offshore wind turbine rotors, Wind Energy, 18, 835–850, https://doi.org/10.1002/we.1733, 2015b.

Chaviaropoulos, P. K. and Sieros, G.: Design of Low Induction Rotors for use in large offshore wind farms, Ewea 2014, pp. 51–55, 2014.

Fleming, P. A., Ning, A., Gebraad, P. M. O., and Dykes, K.: Wind plant system engineering through optimization of layout and yaw control, Wind Energy, 19, 329–344, https://doi.org/10.1002/we.1836, 2016.

Kelley, C. L.: Optimal Low-Induction Rotor Design, in: Wind Energy Science Conference 2017, 2017.

Millman, K. J. and Aivazis, M.: Python for scientists and engineers, Computing in Science and Engineering, 13, 9–12, https://doi.org/10.1109/MCSE.2011.36, 2011.

Perez-Moreno, S. S., Zaaijer, M. B., Bottasso, C. L., Dykes, K., Merz, K. O., Réthoré, P. E., and Zahle, F.: Roadmap to the multidisciplinary design analysis and optimisation of wind energy systems, Journal of Physics: Conference Series, 753, https://doi.org/10.1088/1742-6596/753/6/062011, 2016.

Sieros, G., Chaviaropoulos, P., Sørensen, J. D., Bulder, B. H., and Jamieson, P.: Upscaling wind turbines: theoretical and practical aspects and their impact on the cost of energy, Wind Energy, 15, 3–17, https://doi.org/10.1002/we.527, 2012.

Sørensen, J. N.: The general momentum theory, vol. 4, https://doi.org/10.1007/978-3-319-22114-4_4, 2016.

Zahle, F., Tibaldi, C., Verelst, D. R., Bitche, R., and Bak, C.: Aero-Elastic Optimization of a 10 MW Wind Turbine, https://doi.org/10.2514/6.2015-0491, 2015.

Zhu, C., Byrd, R. H., Lu, P., and Nocedal, J.: Algorithm 778: L-BFGS-B: Fortran subroutines for large-scale bound-constrained optimization, ACM Transactions on Mathematical Software, 23, 550–560, https://doi.org/10.1145/279232.279236, 1997.